Metastability Alloy Design

D. Raabe, D. Ponge

Max-Planck-Institut
für Eisenforschung GmbH
Düsseldorf, Germany

MAX-PLANCK-GESELLSCHAFT

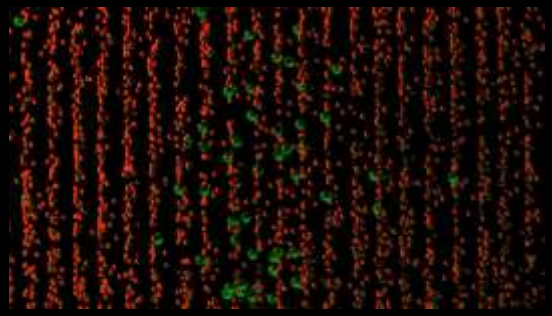

Outline

1. What is Metastability Alloy Design and Segregation Engineering ?

2. How is it done ?

What is Metastability Alloy Design and Segregation Engineering

Chemo-mechanical metastability of crystalline phases

Displacive phase transformation under load

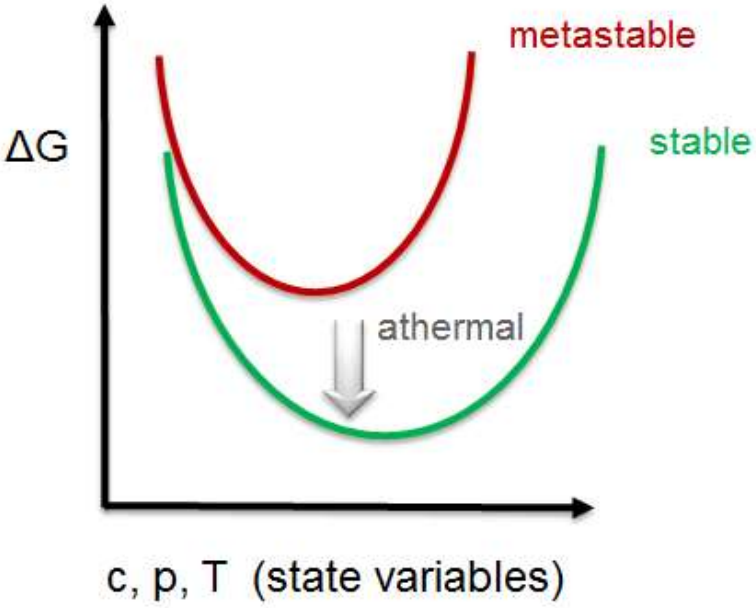

Plastic deformation and strength through dislocation slip

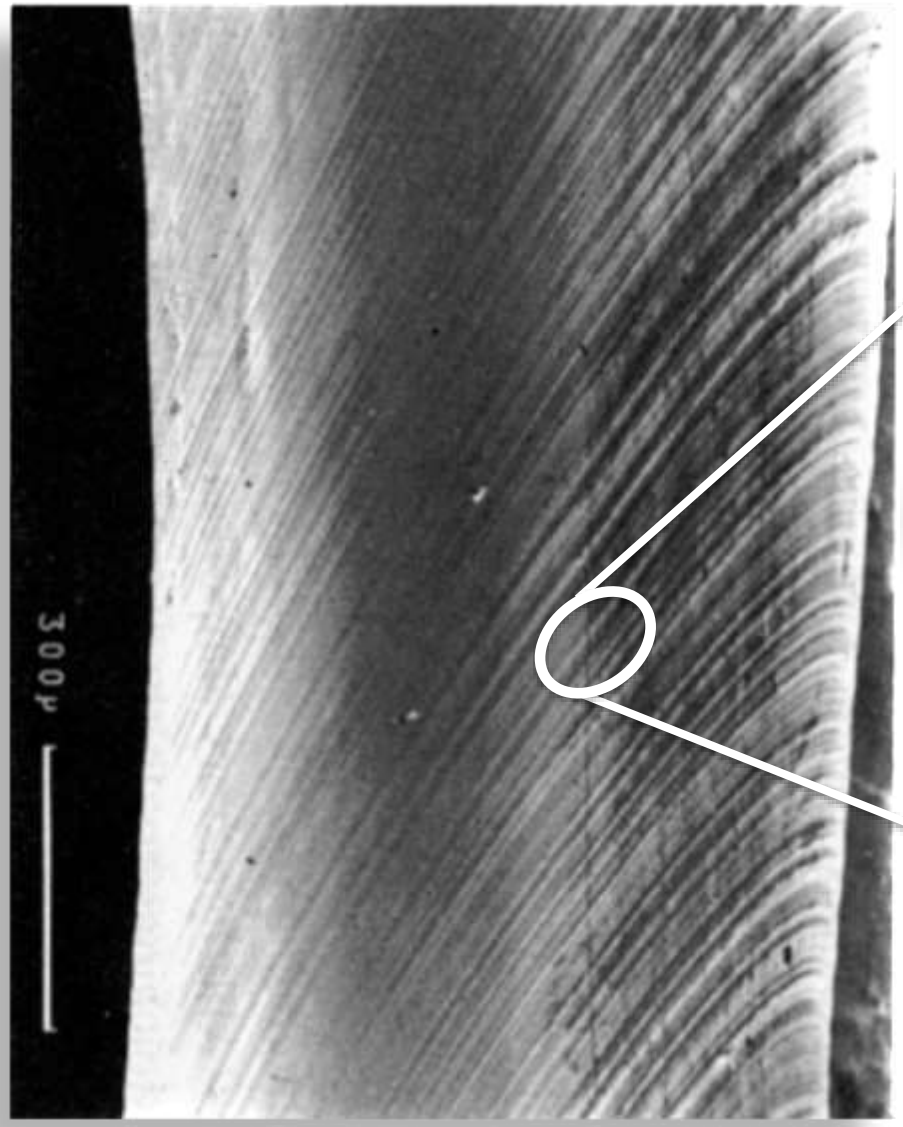

TEM: J. Kacher

Associated strengthening mechanisms

Athermal transformations not affine, not commensurate - high misfit deformation

Multiple strain hardening effects

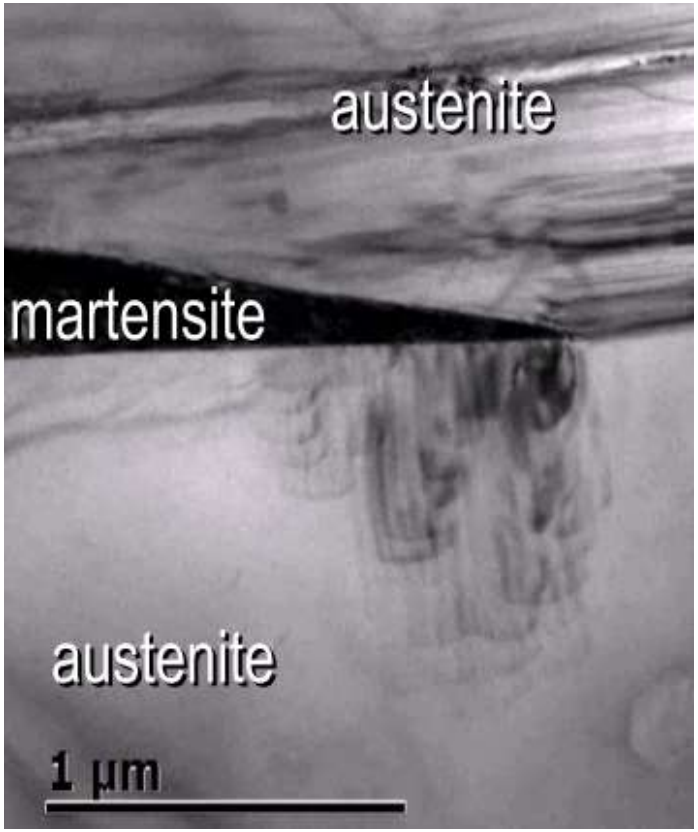

What is Metastability Alloy Design and Segregation Engineering

Chemo-mechanical **metastability** of crystals

Displacive phase **transformation** under load

Confined at lattice defects using chemical and size effects

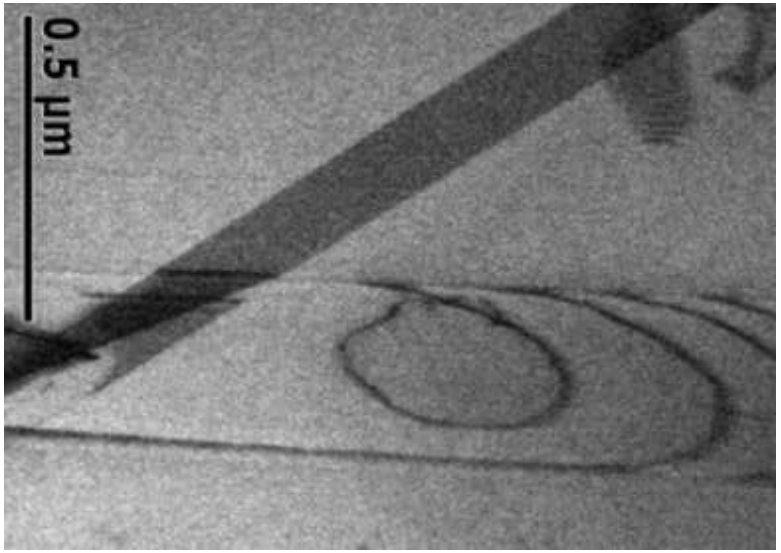

Outline

1. What is Metastability Alloy Design and Segregation Engineering ?

2. How is it done ?

1. What is Metastability Alloy Design and Segregation Engineering ?

2. **How is it done ?**

- **Bulk: tune barriers & transformation driving forces**
- **Confinement to lattice defects**
  Segregation & local displacive transformation

Metastability Alloy Design

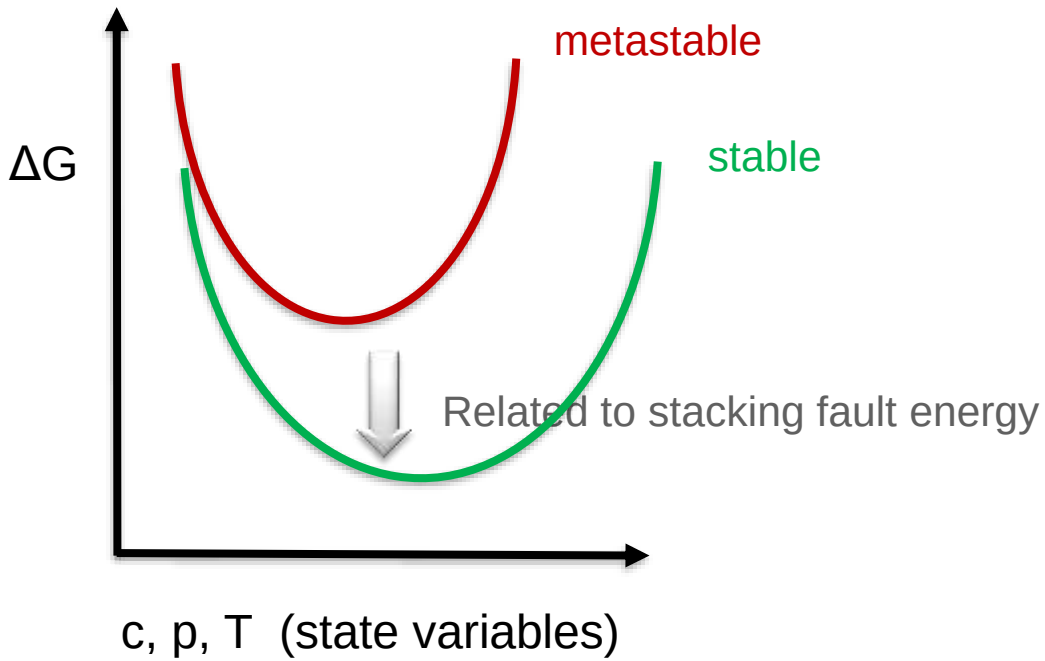

- **Bulk: tune barriers & transformation driving forces**
- **Confinement to lattice defects**
  Segregation & local displacive transformation

Bulk metastability FCC alloy design: tune stacking fault energy

lower SFE →

high-Mn (15-30%), HEA

γ (fcc) cells → γ (fcc) planar → γ (fcc+order) planar → γ (fcc+twins) → ε (hcp) → α' (bcc/ bct)

high-Mn+Al

medium-Mn (5-12%)

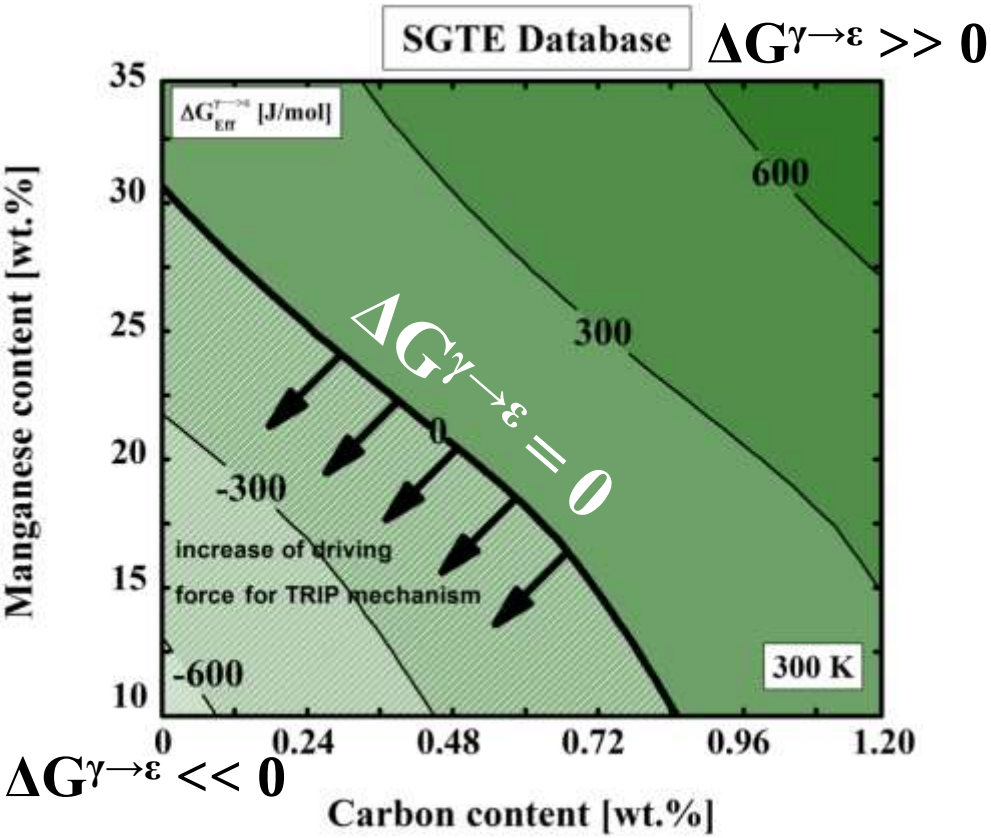

Critical stress for twin growth:

$$\tau_c = \frac{\gamma_{sf}}{3b_s} + \frac{3Gb_s}{L_0}$$

Critical stress for ε-martensite growth:

$$\tau_c = \frac{\gamma_{sf}}{3b_s} + \frac{3Gb_s}{L_0} + \frac{h\Delta G^{\gamma\to\varepsilon}}{3b_s}$$

Values of SFEs: D. Pierce, Acta Mater 68 (2014)

Steinmetz et al. Acta Mater 61 (2013), Wong et al. Acta Mater 118 (2016)

Inverse strength-ductility: phenomenological analysis

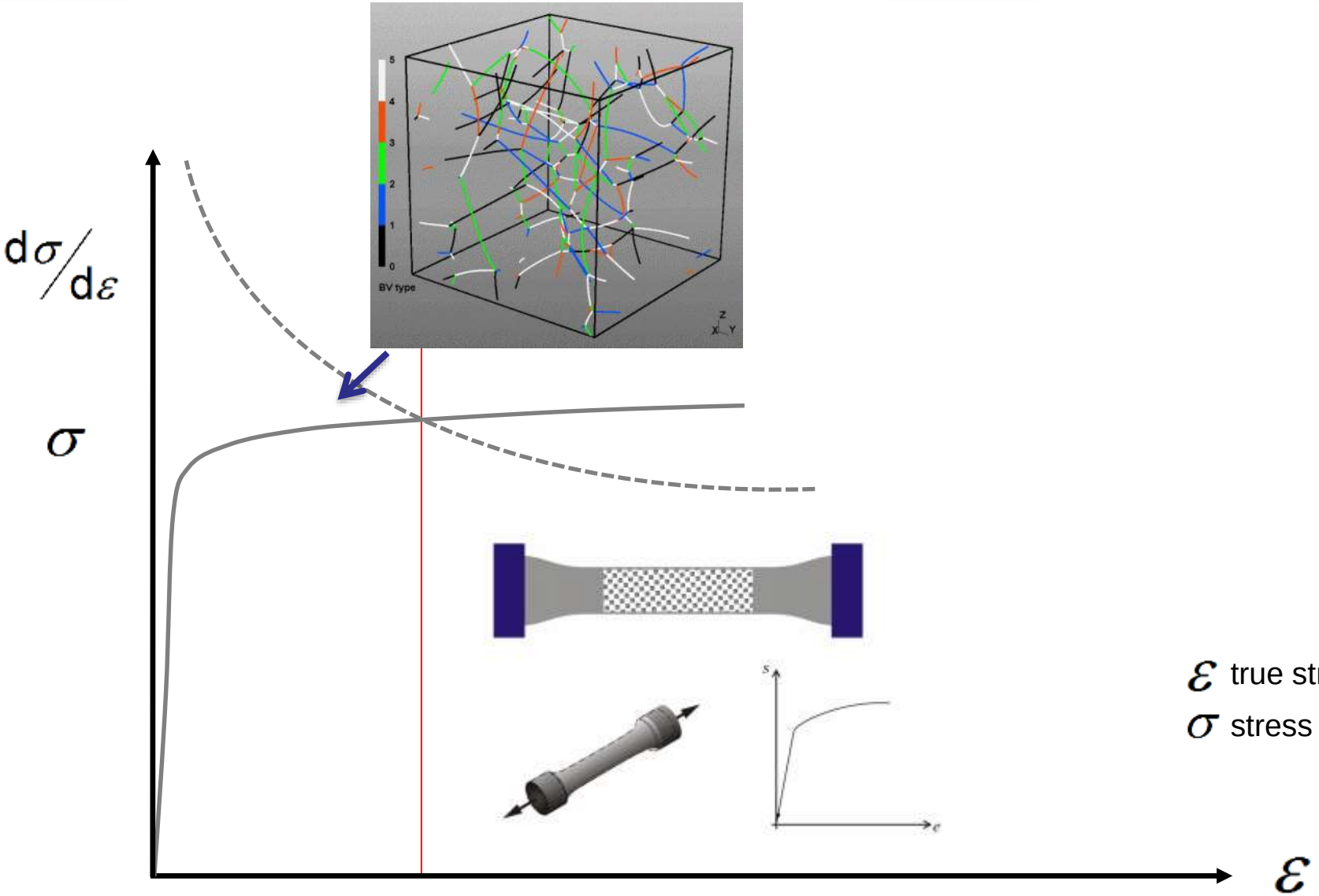

Inverse strength-ductility: phenomenological analysis

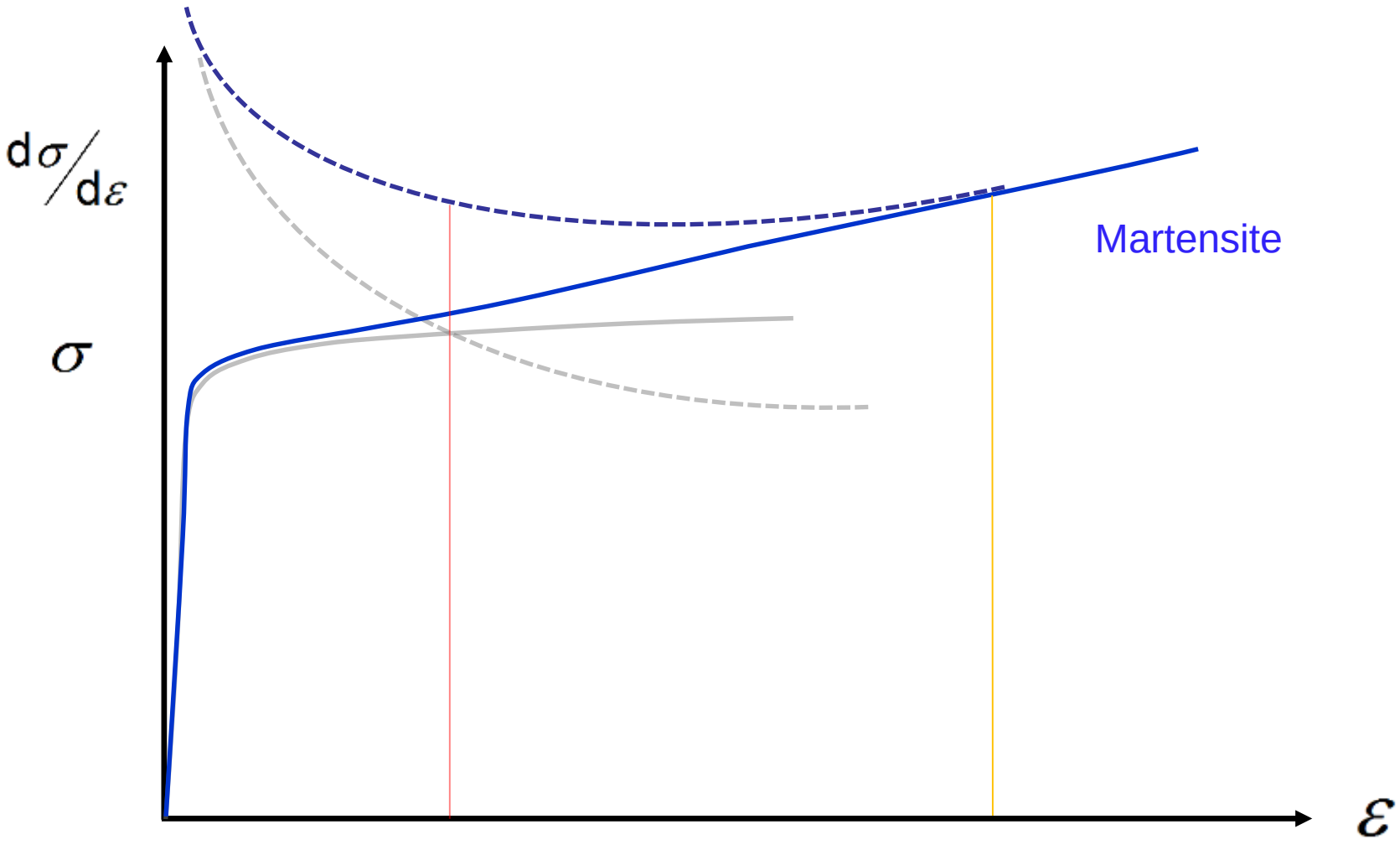

Inverse strength-ductility: phenomenological analysis

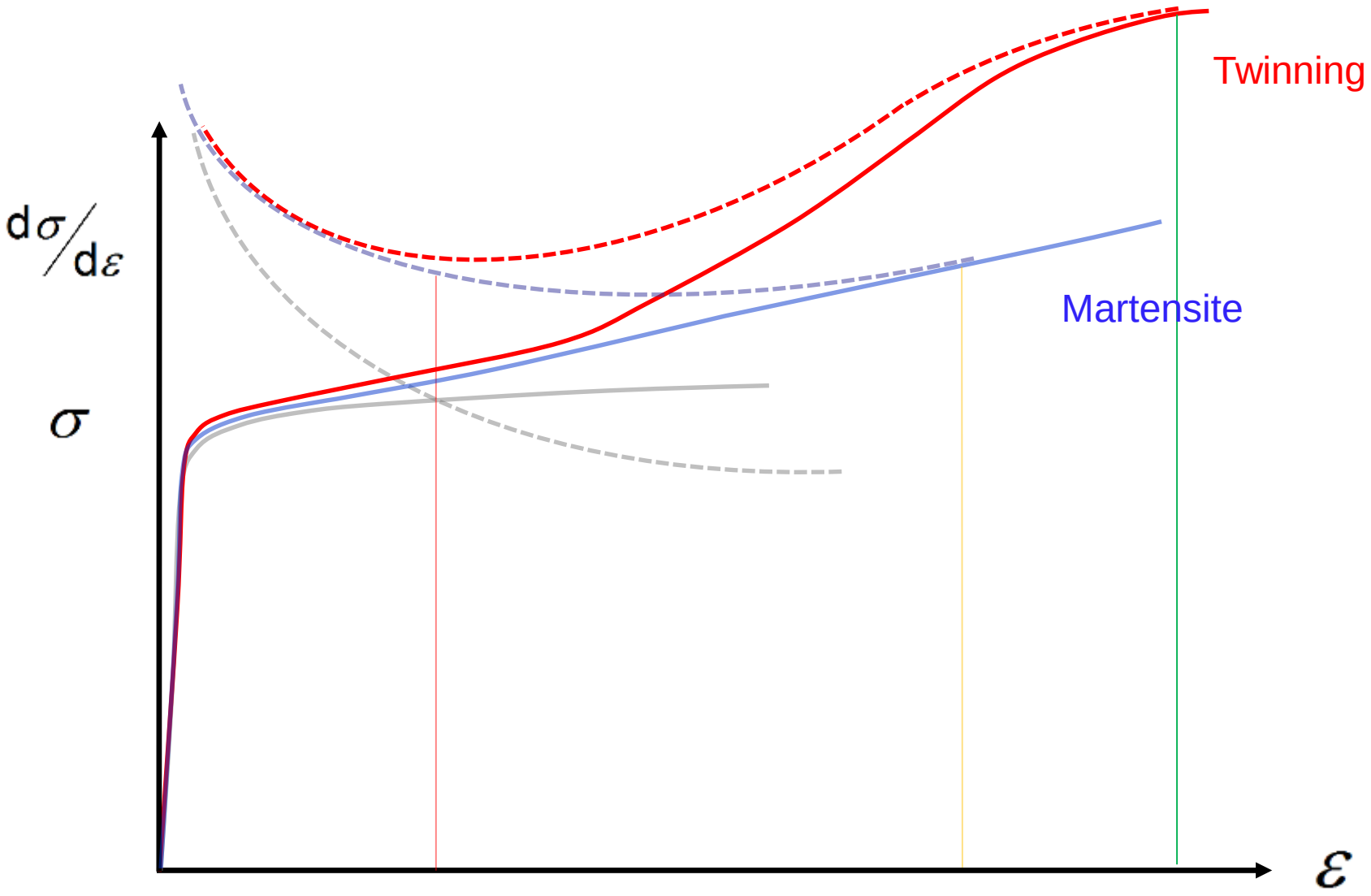

Inverse strength-ductility: phenomenological analysis

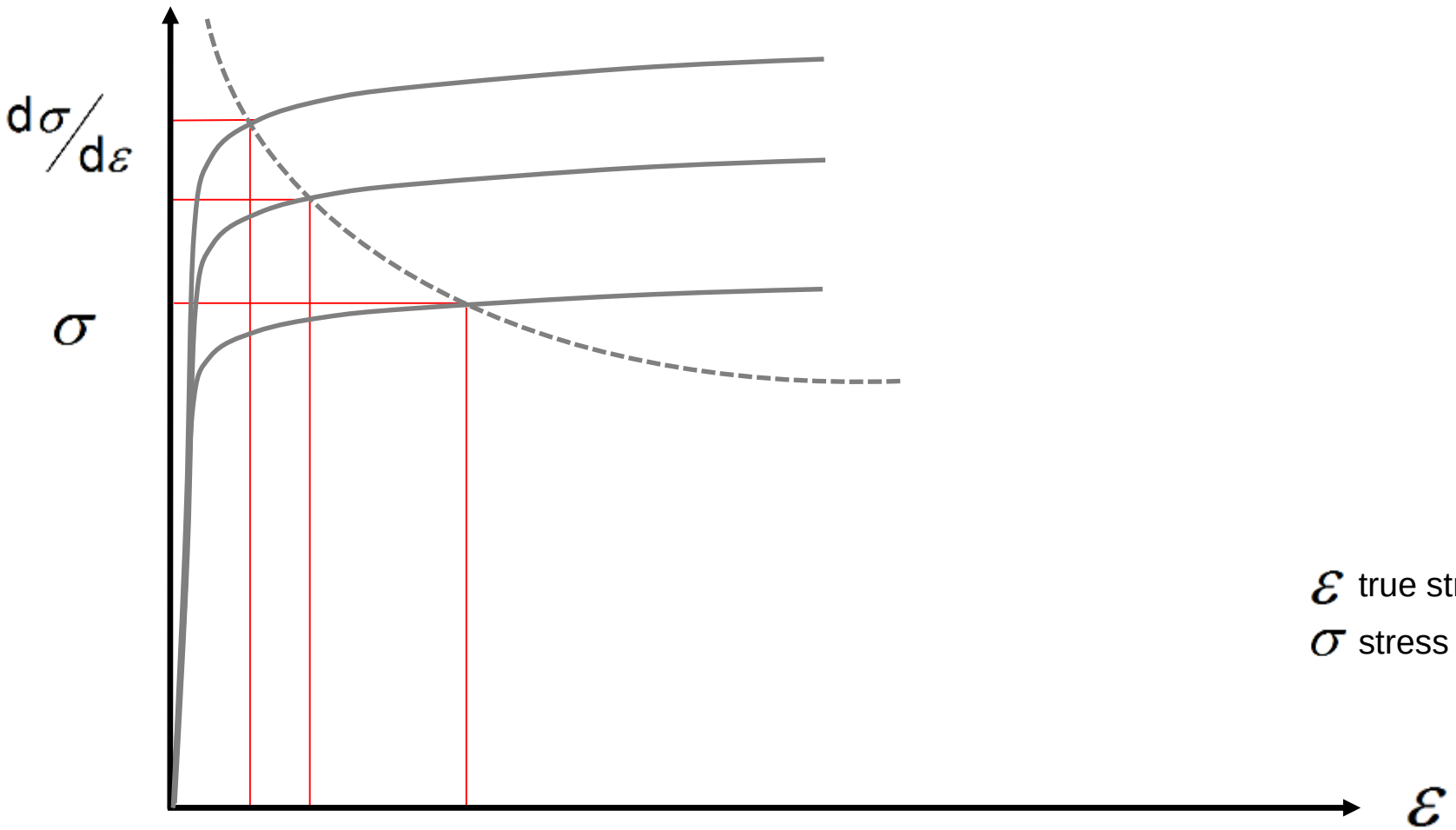

ε true strain

σ stress

Metastability and segregation design: strengthening mechanisms

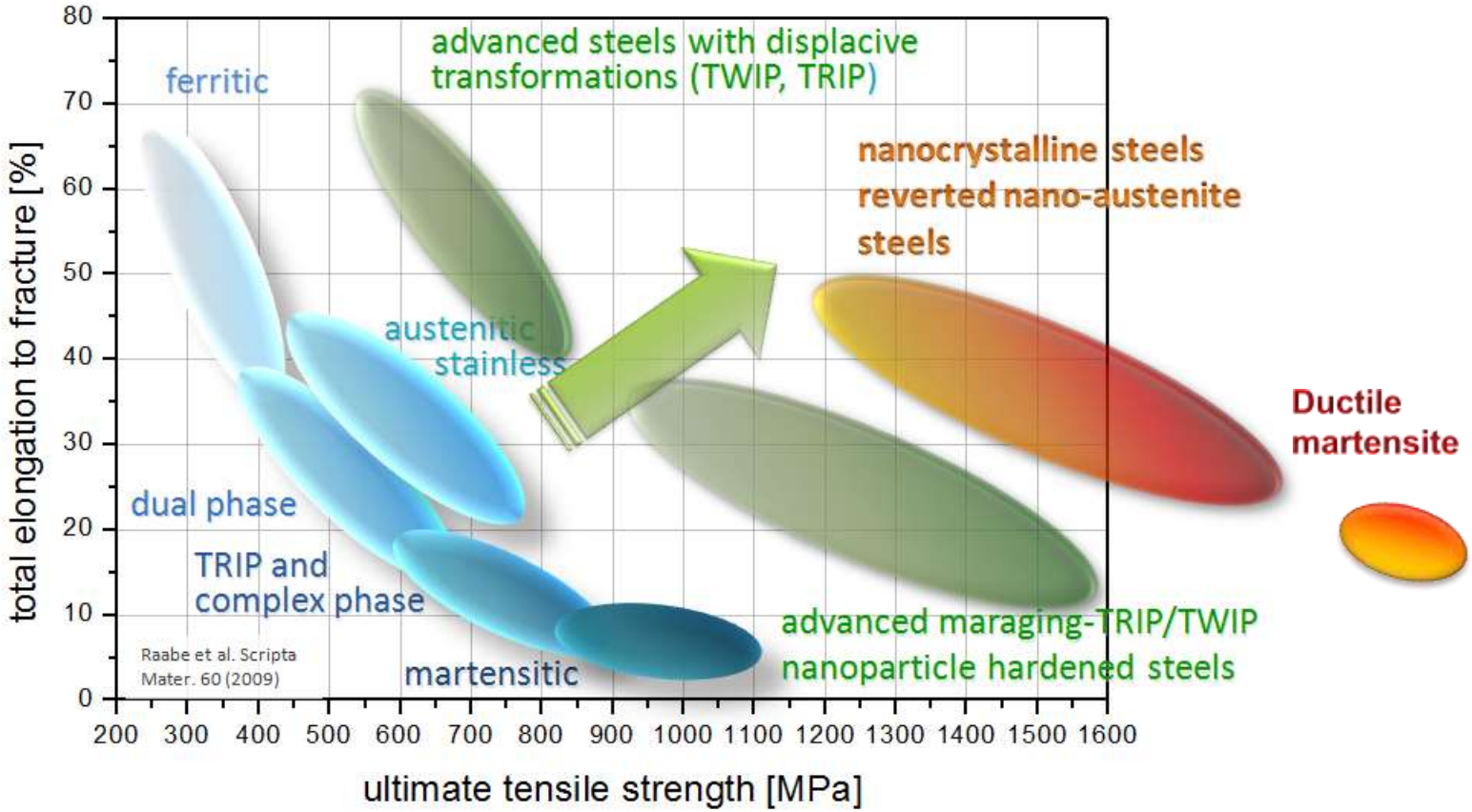

Raabe et al. Scripta Mat 60 (2009); Wen et al. Nature Com (2014)

Metastability Alloy Design: strengthening mechanisms

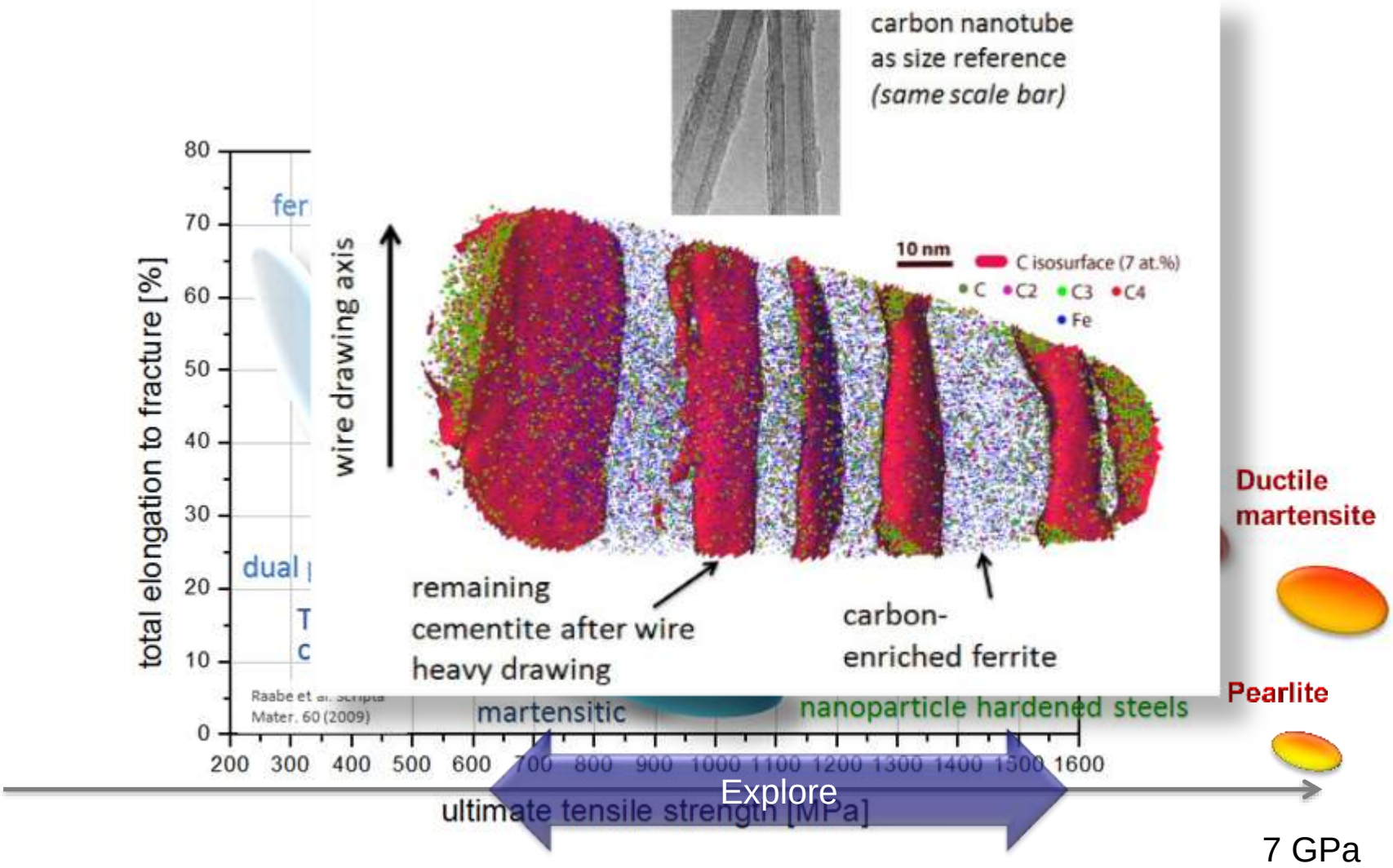

Li et al. PRL (2014); Herbig et al. PRL (2014); Wen et al. Nature Com 2014

Bulk Metastability Alloy Design: Fe-22Mn-0.6C TWIP steel (wt.%)

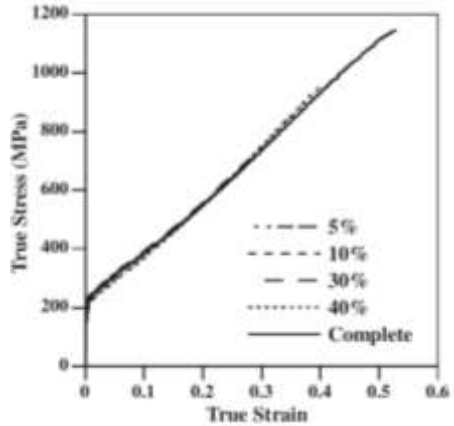

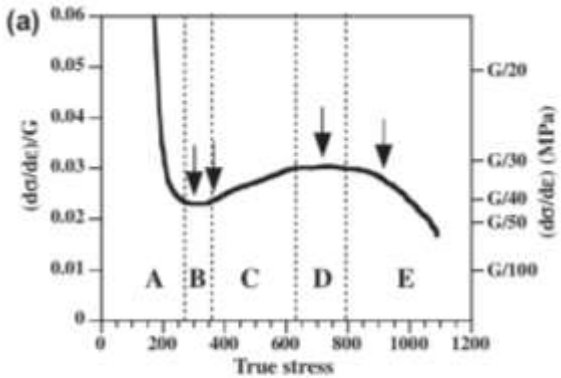

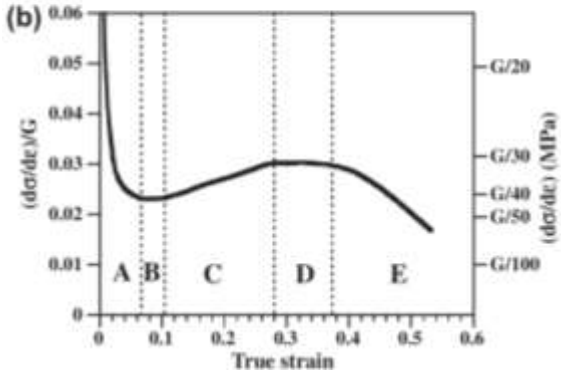

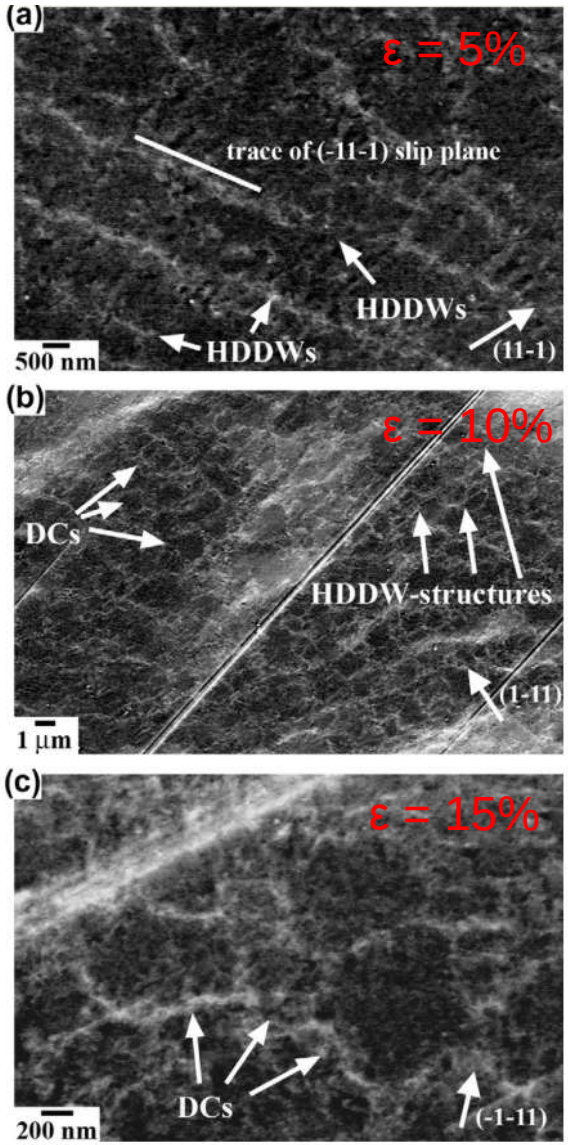

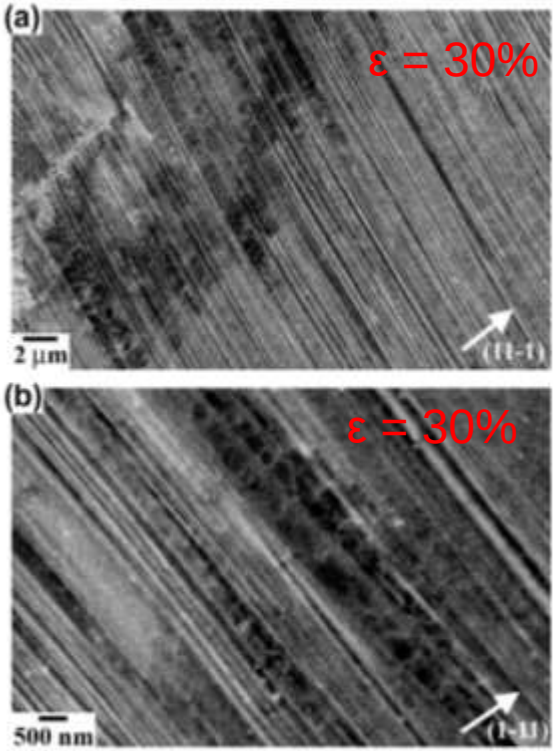

Gutierrez-Urrutia et al. (2012) Acta Mater. 60, p. 5791; (2011) 59, p. 6449

Bulk Metastability Alloy Design: Fe-Mn-Al-C solid solution

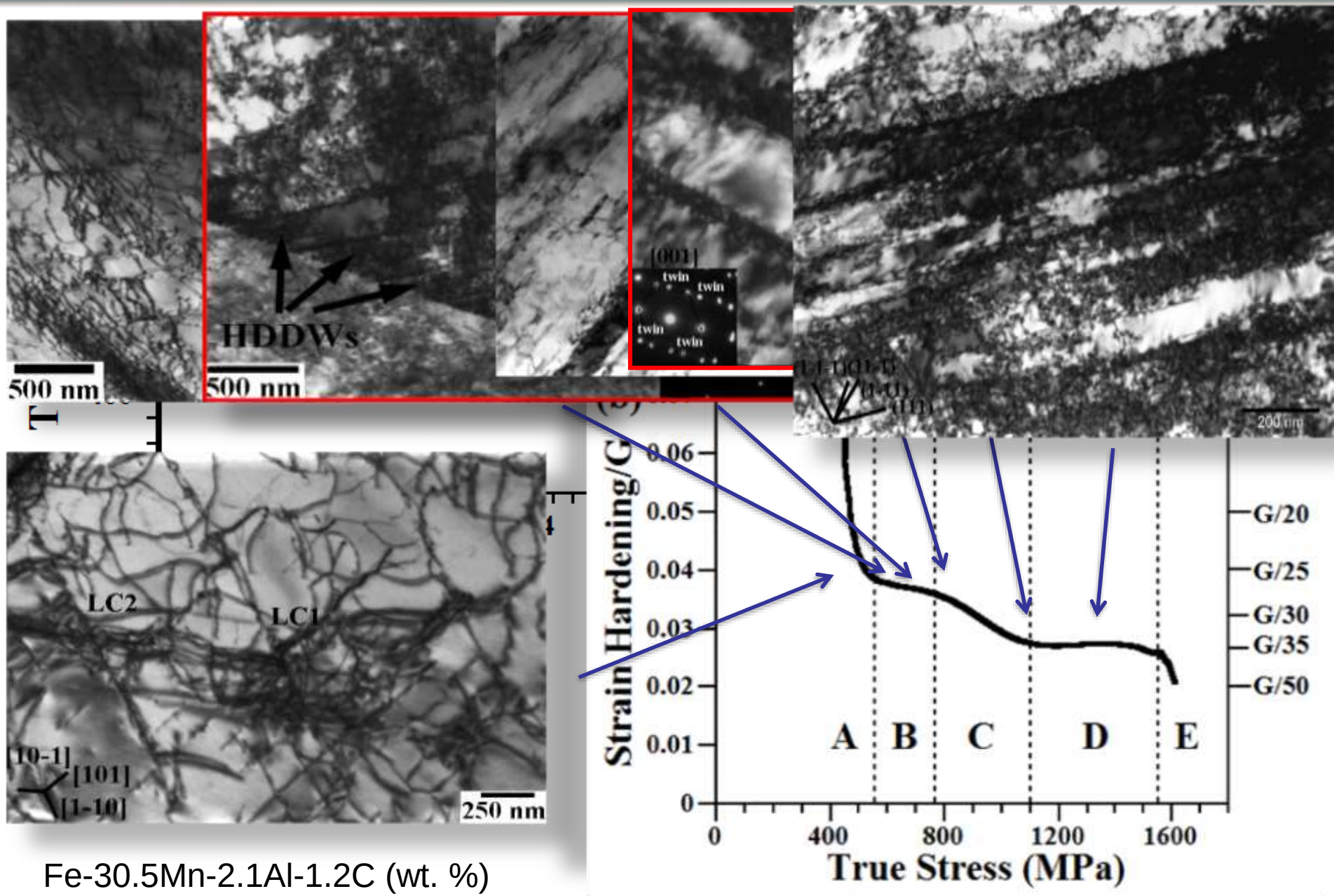

Fe-30.5Mn-2.1Al-1.2C (wt. %)

Gutierrez-Urrutia, et al . Acta Materialia 60 (2012) 5791

Motivation for non-equiatiomic HEAs: FeMnNiCoCr (Cantor alloy)

Not only driven by config. entropy
Flat entropy curve

Phase stability and SFE
Drop single phase rule

Bulk Rapid Alloy Protoyping: RAP
Property maps

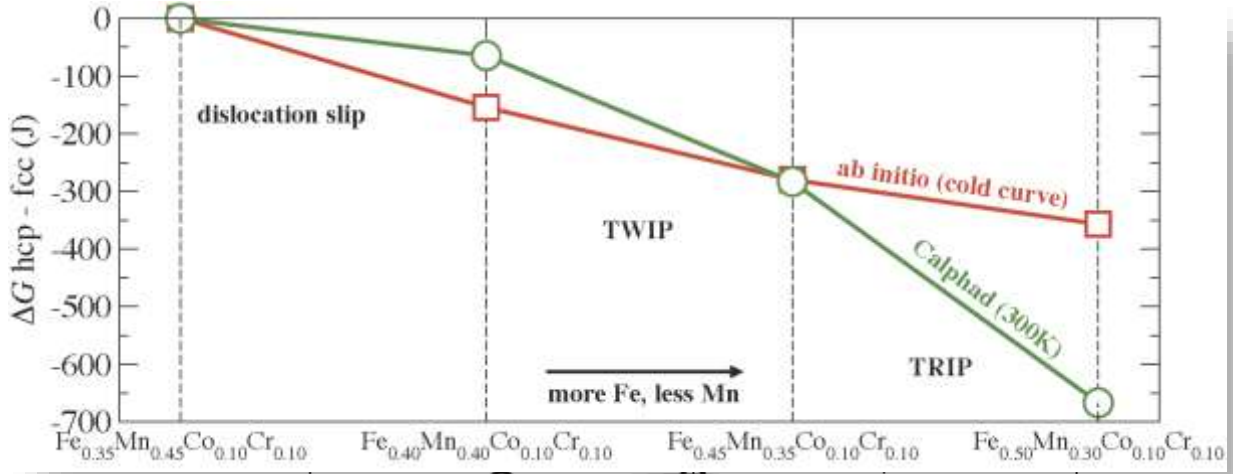

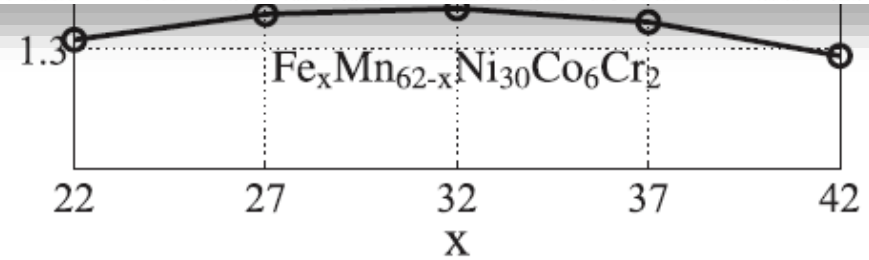

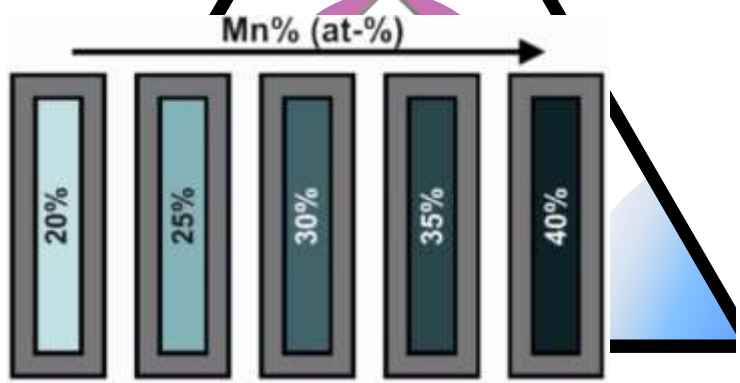

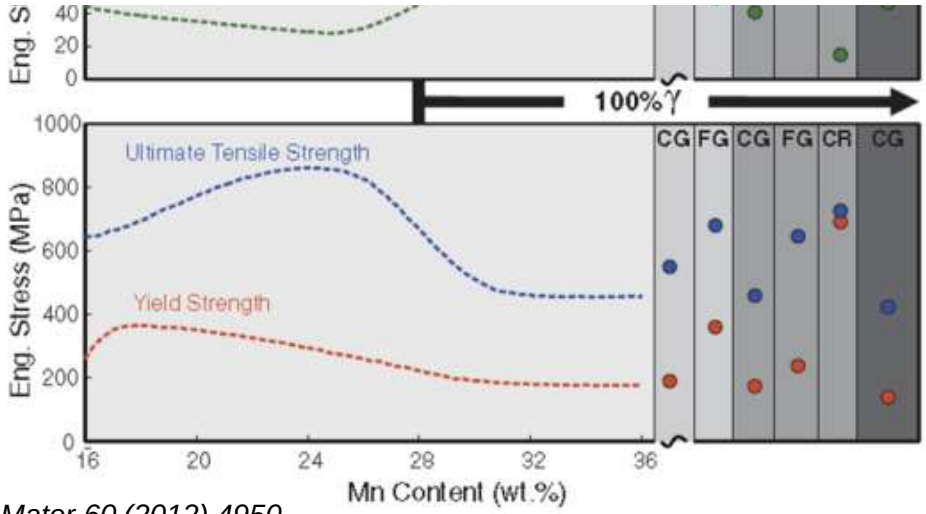

H. Springer et al. Acta Mater.60 (2012) 4950

D. Ma et al. Acta Mater.100 (2015) 90

Example: Fe-Mn-Al-C alloys – 10-18% weight reduction

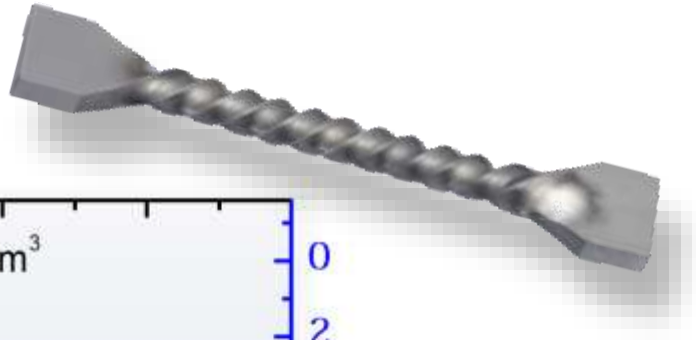

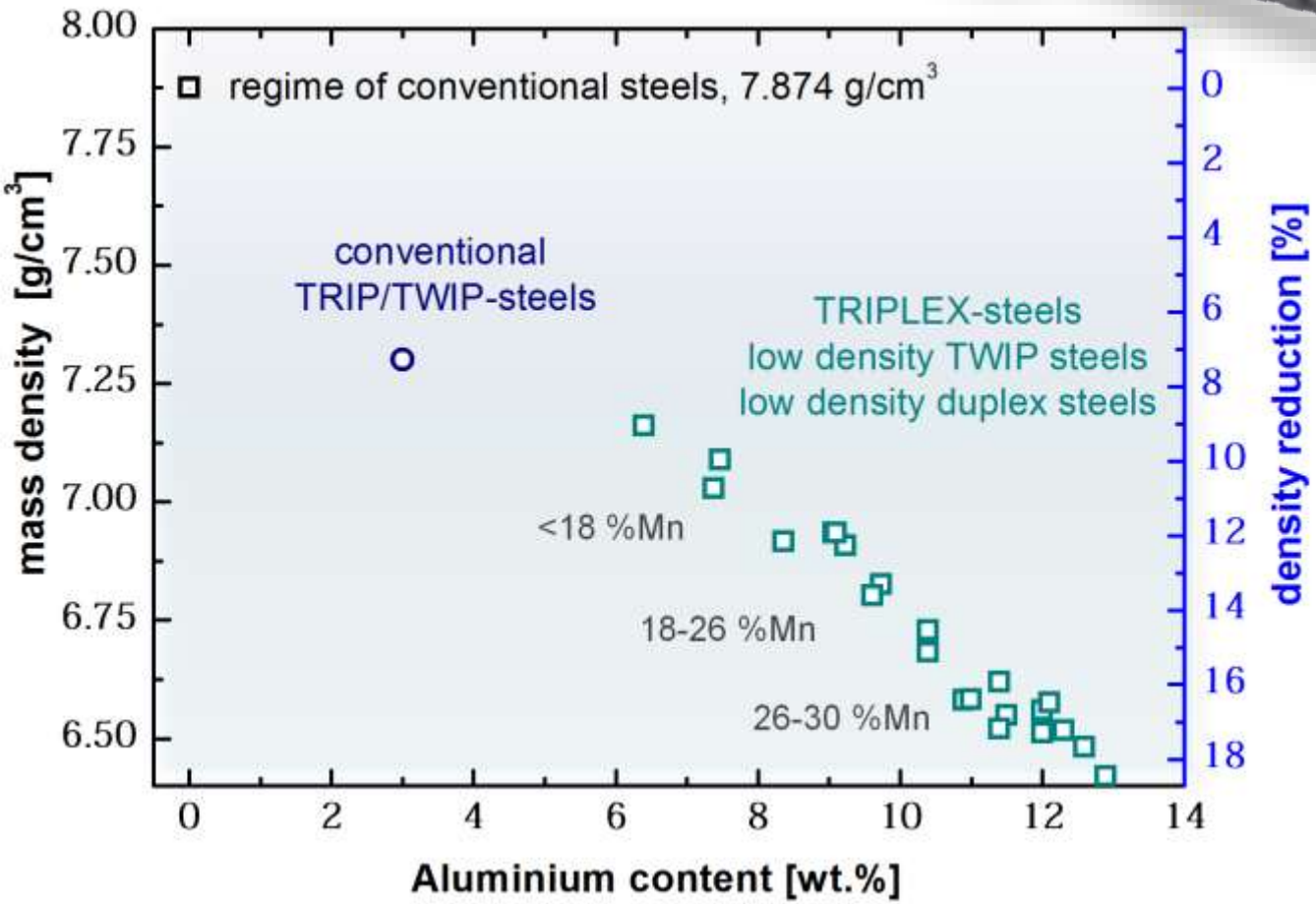

Yao et al. Acta Mater. 106 (2016) 229; Raabe et al. Steel Res. 86 (2015)

Fe-30Mn-8Al-1.2C, different annealing times at 600°C

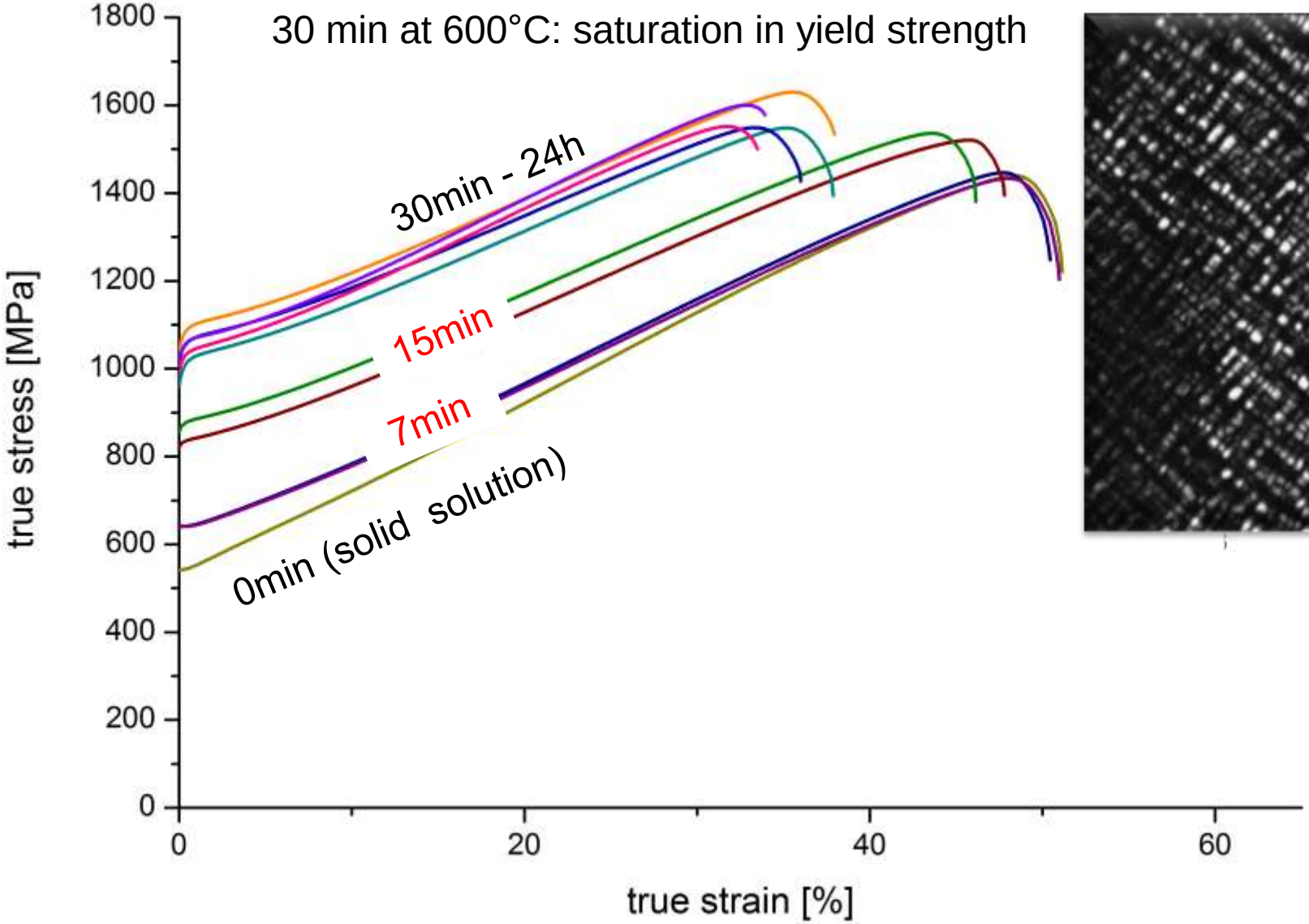

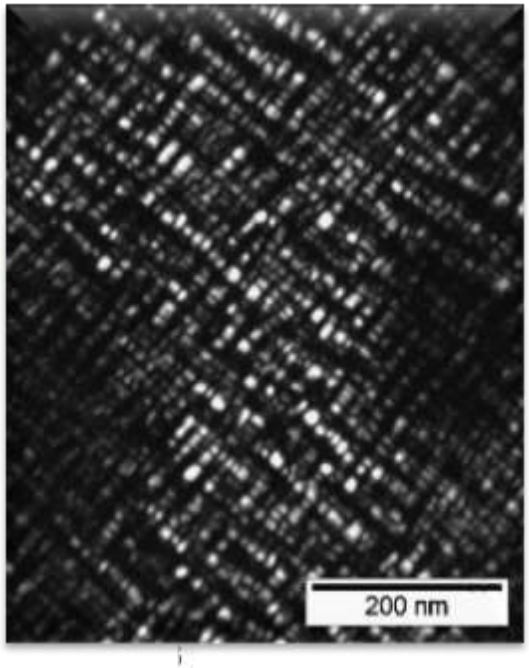

Yao Acta Mater. 106 (2016) and (2017); Welsch (2016) Acta Mater. 116

γ/κ steel Fe-30Mn-8Al-1.2C

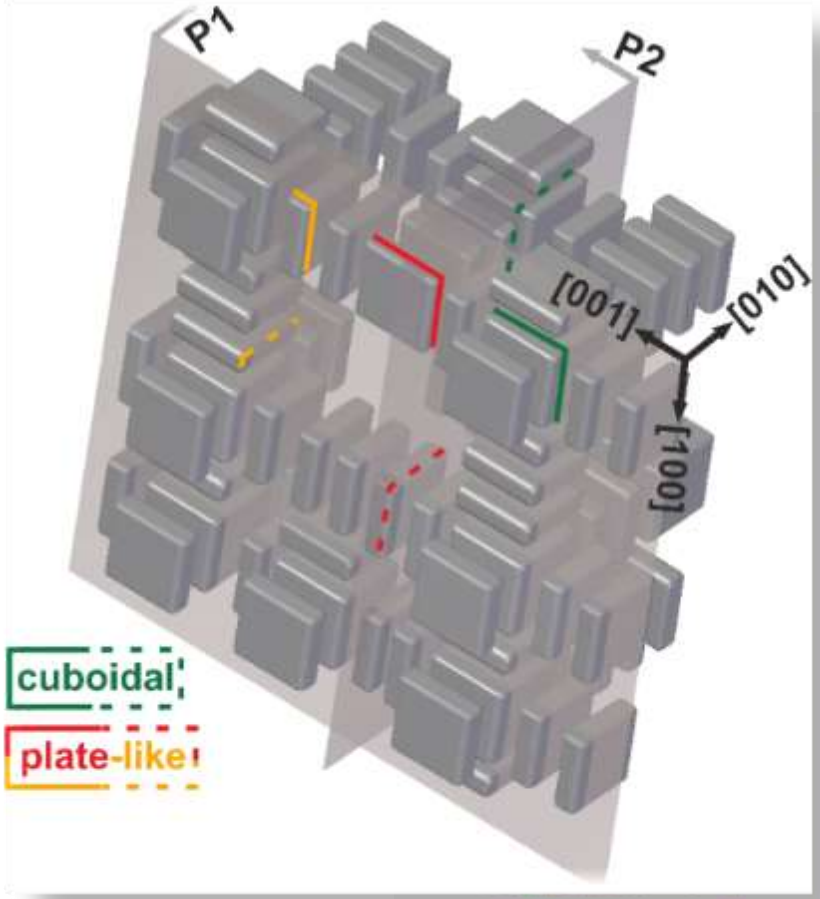

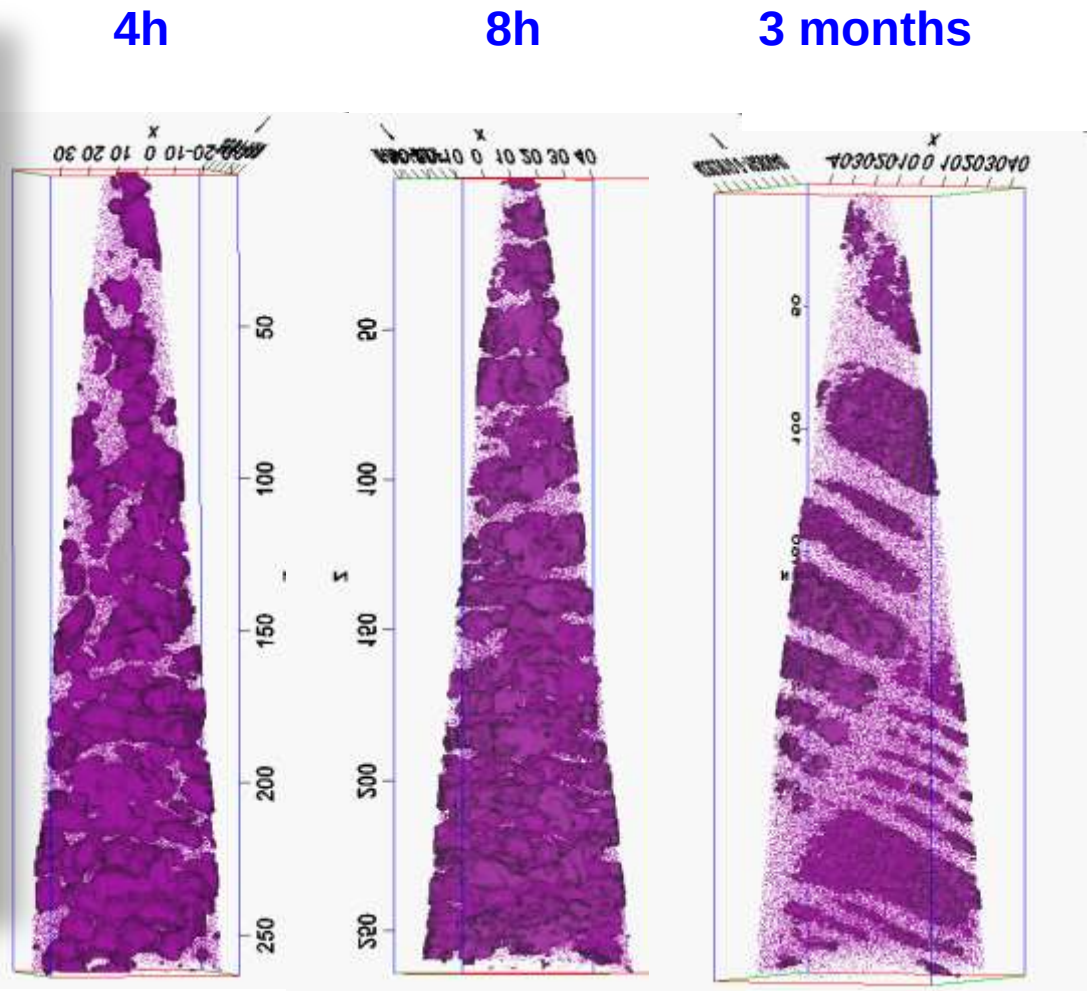

40 nm

•C ▬ ≥ 7.0 at.% C

Yao Acta Mater. 106 (2016) and (2017); Welsch (2016) Acta Mater. 116

Weight reduced steels

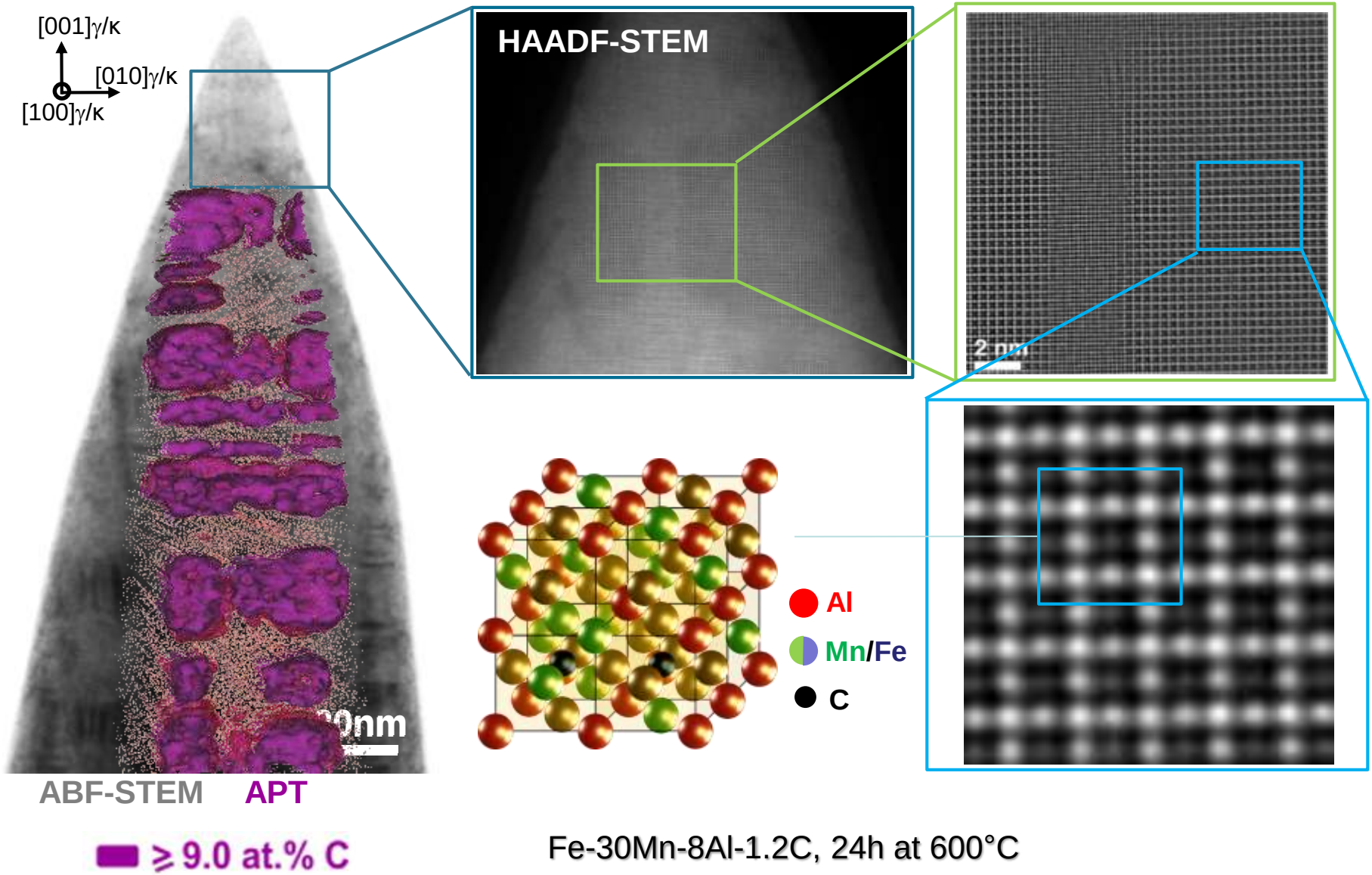

Fe-30Mn-8Al-1.2C, 24h at 600°C

γ/κ steel Fe-30Mn-8Al-1.2C

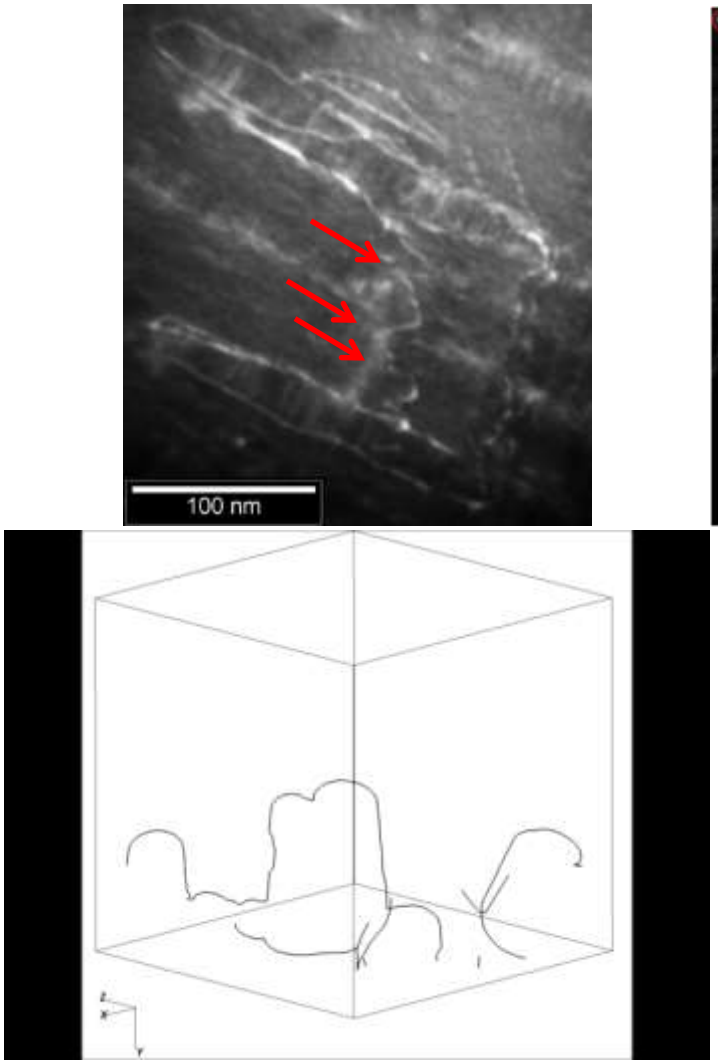

Dislocation pinning due to cross-slip into different conjugate glide plane

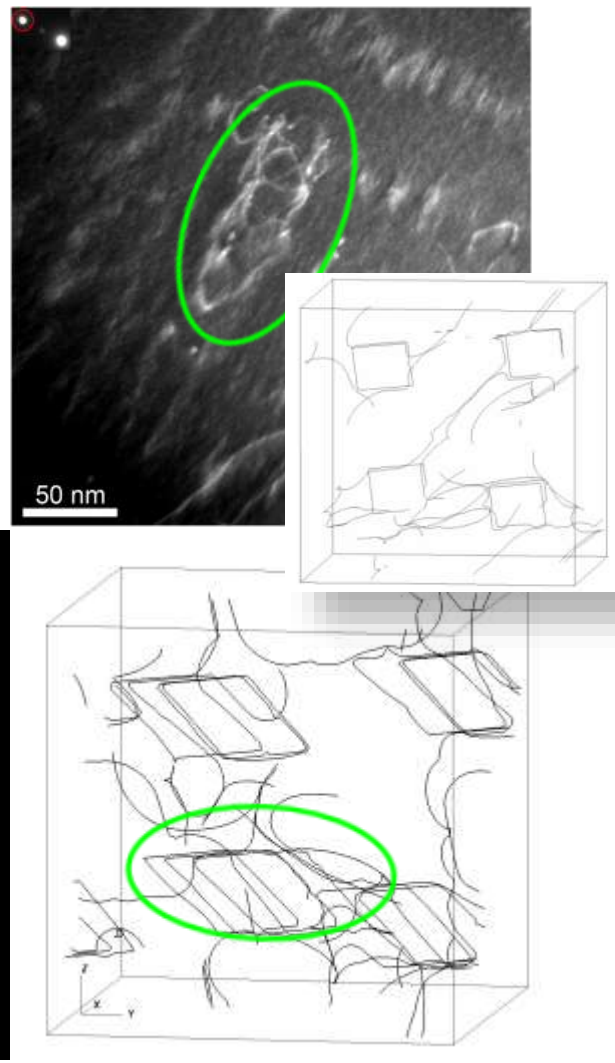

Dislocation wrapping around κ-carbides

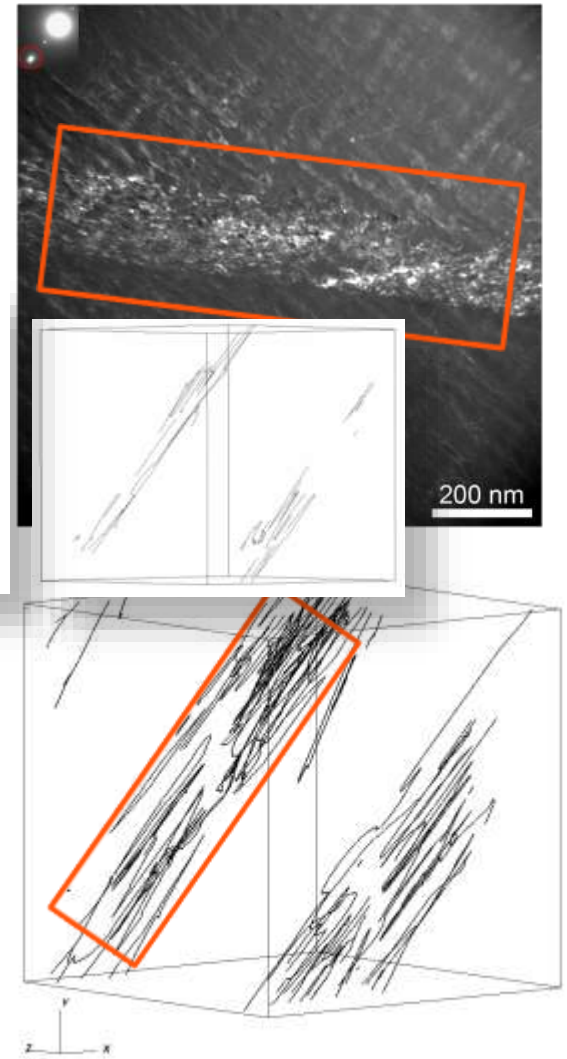

Formation of slip bands from individual dislocation sources

Fe-30Mn-8Al-1.2C, 600°C-24h ε=15%

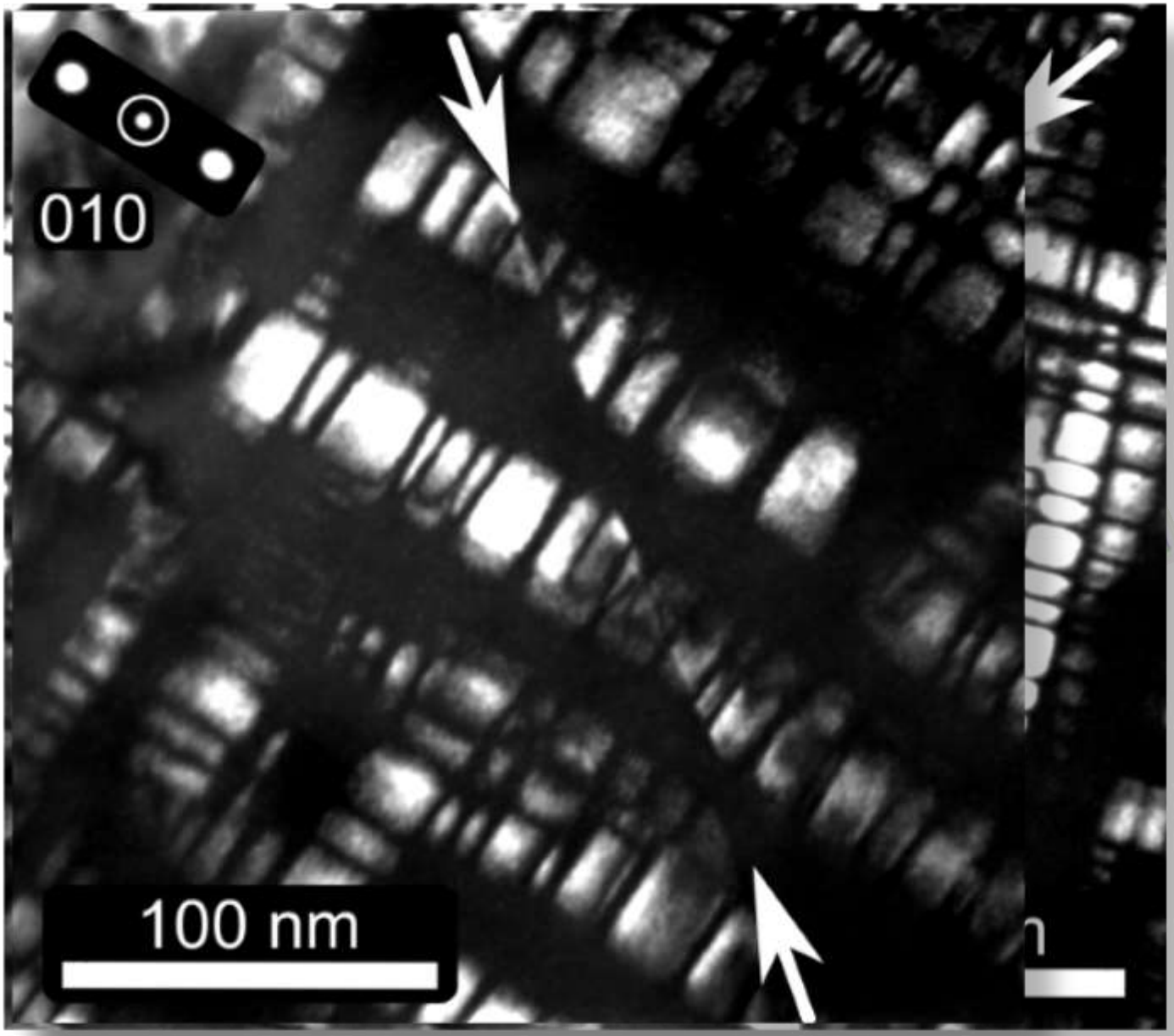

Welsch et al. (2016) Acta Mater. 116, pp. 188: Acta Mater (2017)

Fe-30Mn-8Al-1.2C (wt%), as-quenched, no kappa precipitates

Electron Channeling Contrast Imaging ECCI

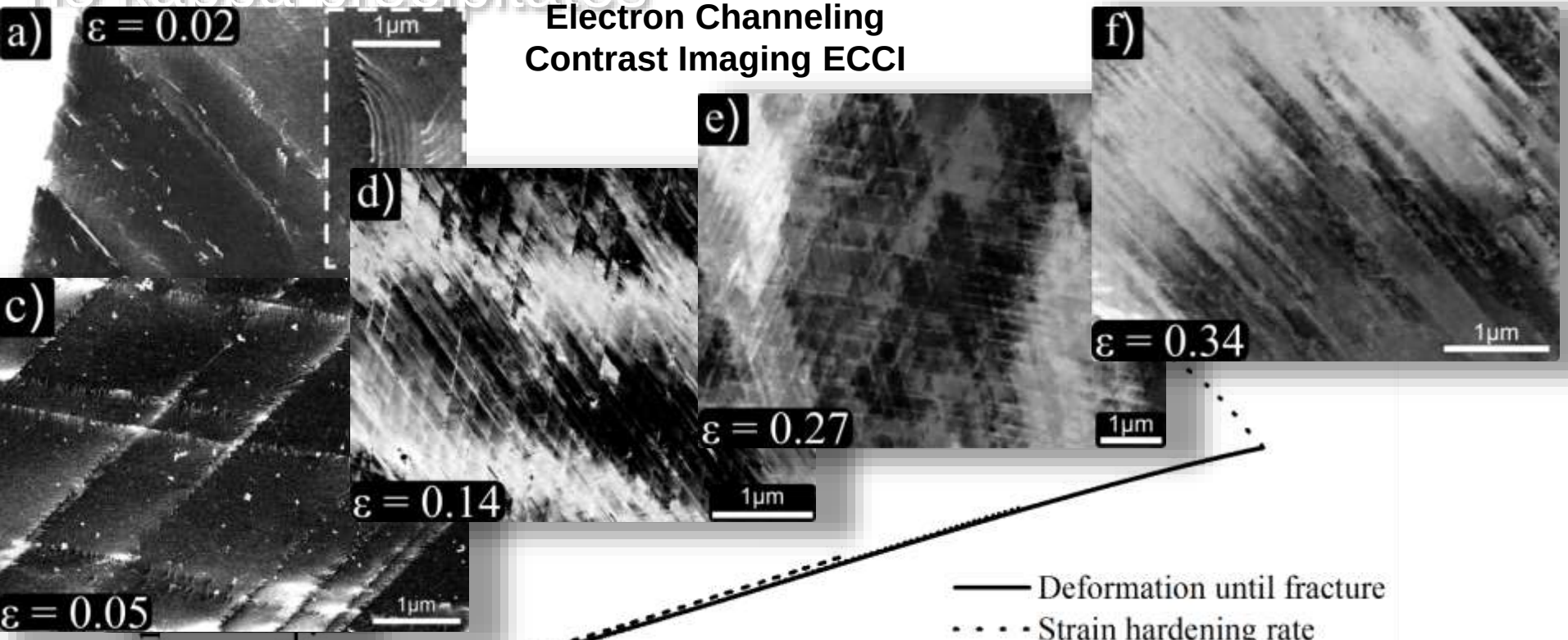

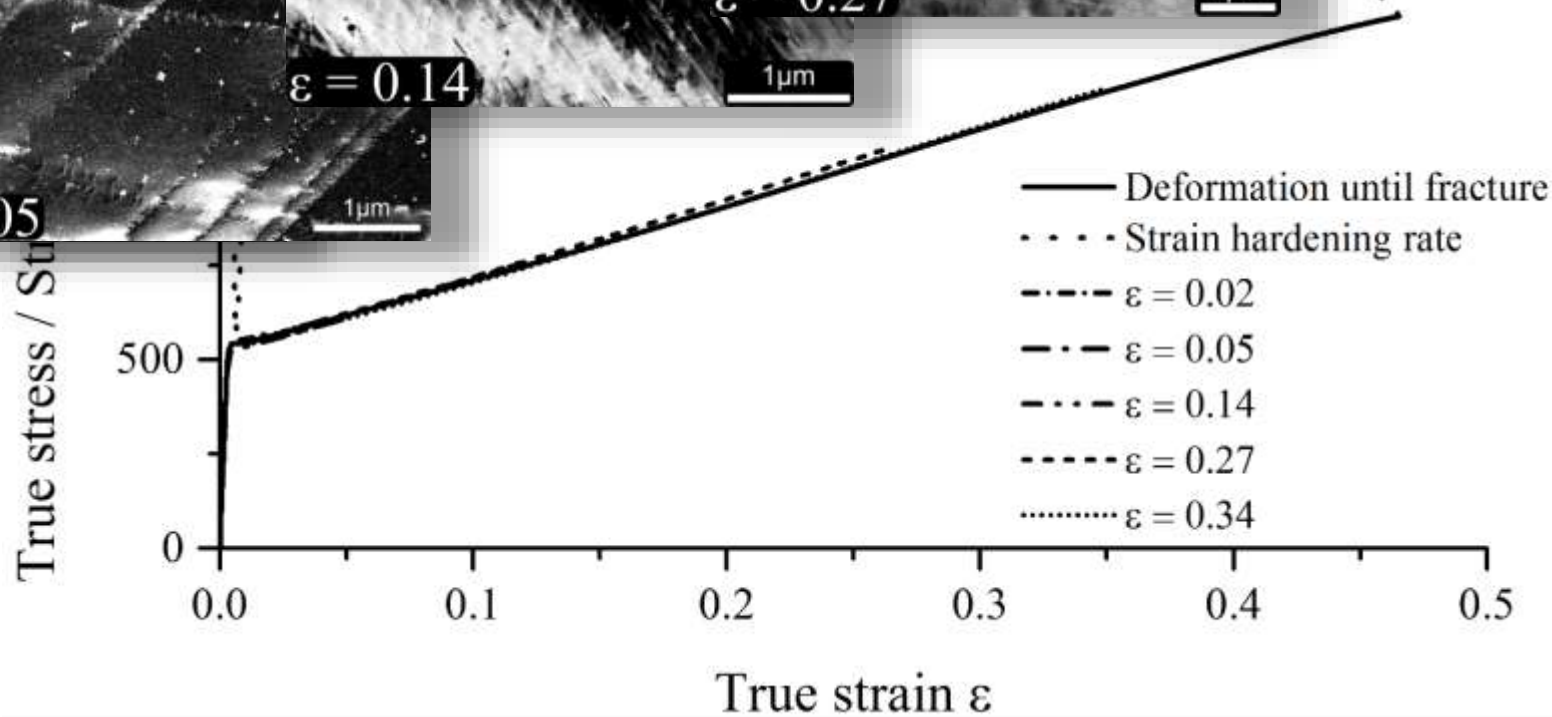

Yao Acta Mater. 106 (2016) 229; Welsch (2016) Acta Mater. 116, pp. 188

Fe-30.4Mn-8Al-1.2C (wt%), as-quenched, no kappa precipitates

Electron Channeling Contrast Imaging ECCI

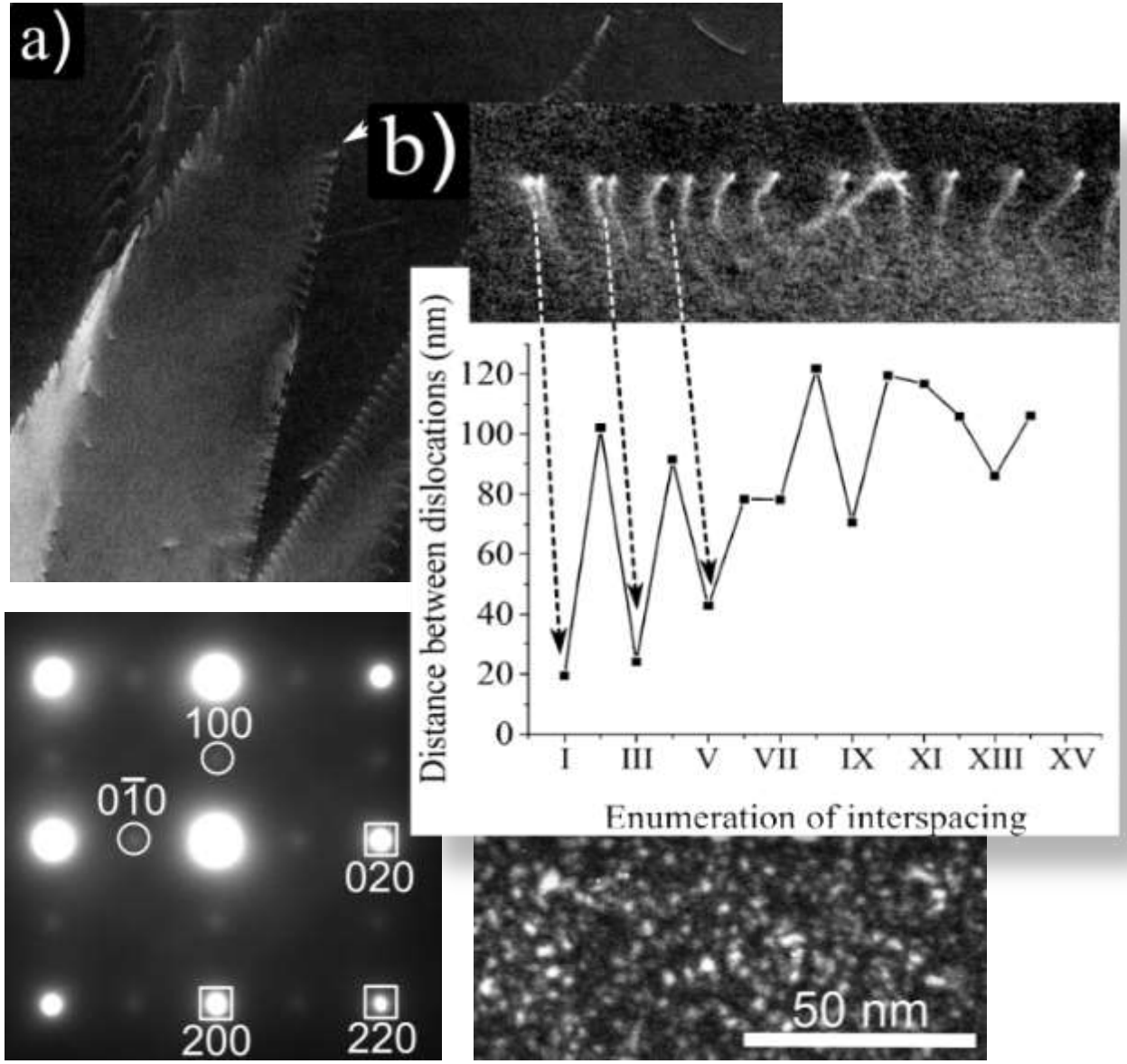

Yao Acta Mater. 106 (2016) 229; Welsch (2016) Acta Mater. 116, pp. 188

Fe-30Mn-8Al-1.2C, 600°C-24h ε=15%

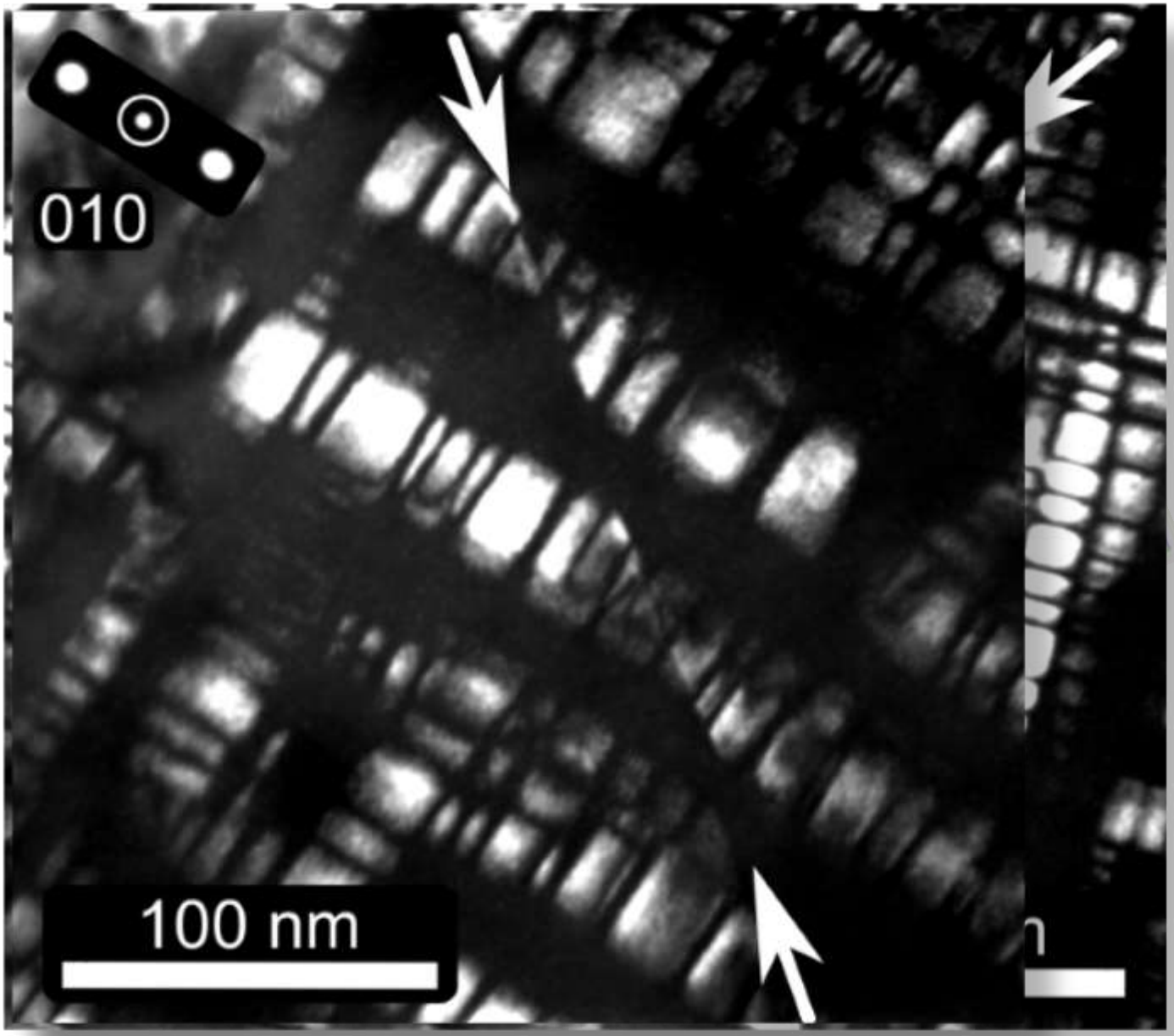

Welsch et al. (2016) Acta Mater. 116, pp. 188: Acta Mater (2017)

γ/κ steel Fe-30Mn-8Al-1.2C

$\sigma_{SH}(\varepsilon) = K \cdot M \cdot G \cdot b/D$

K : geometrical factor

G : 70 GPa

D : mean slip band spacing

M : 3.06 Taylor-factor

b : 0.26 nm

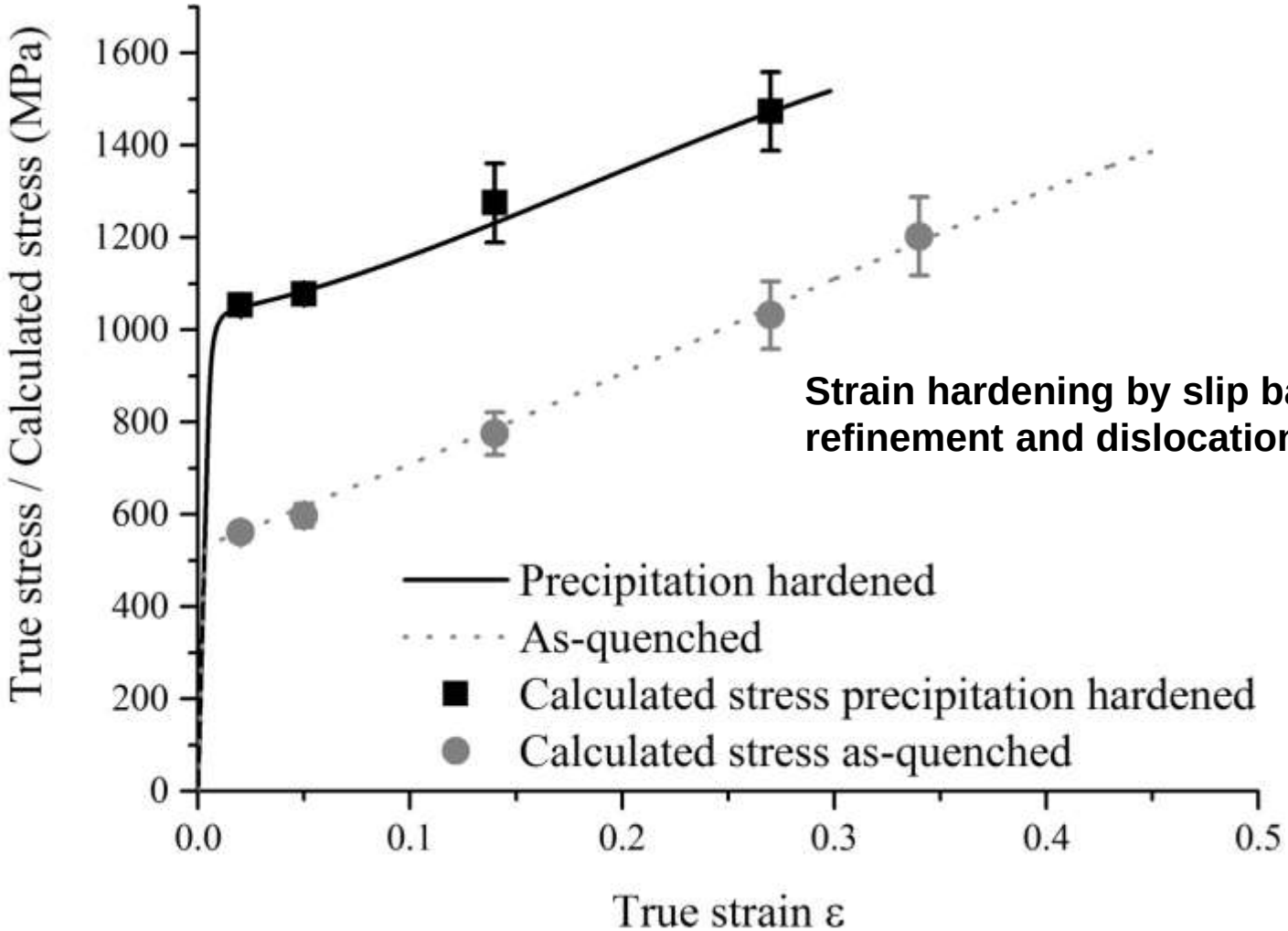

Strain hardening by slip band spacing refinement and dislocation passing stress

Strain rate 800/s: compare TWIP steel to DP800

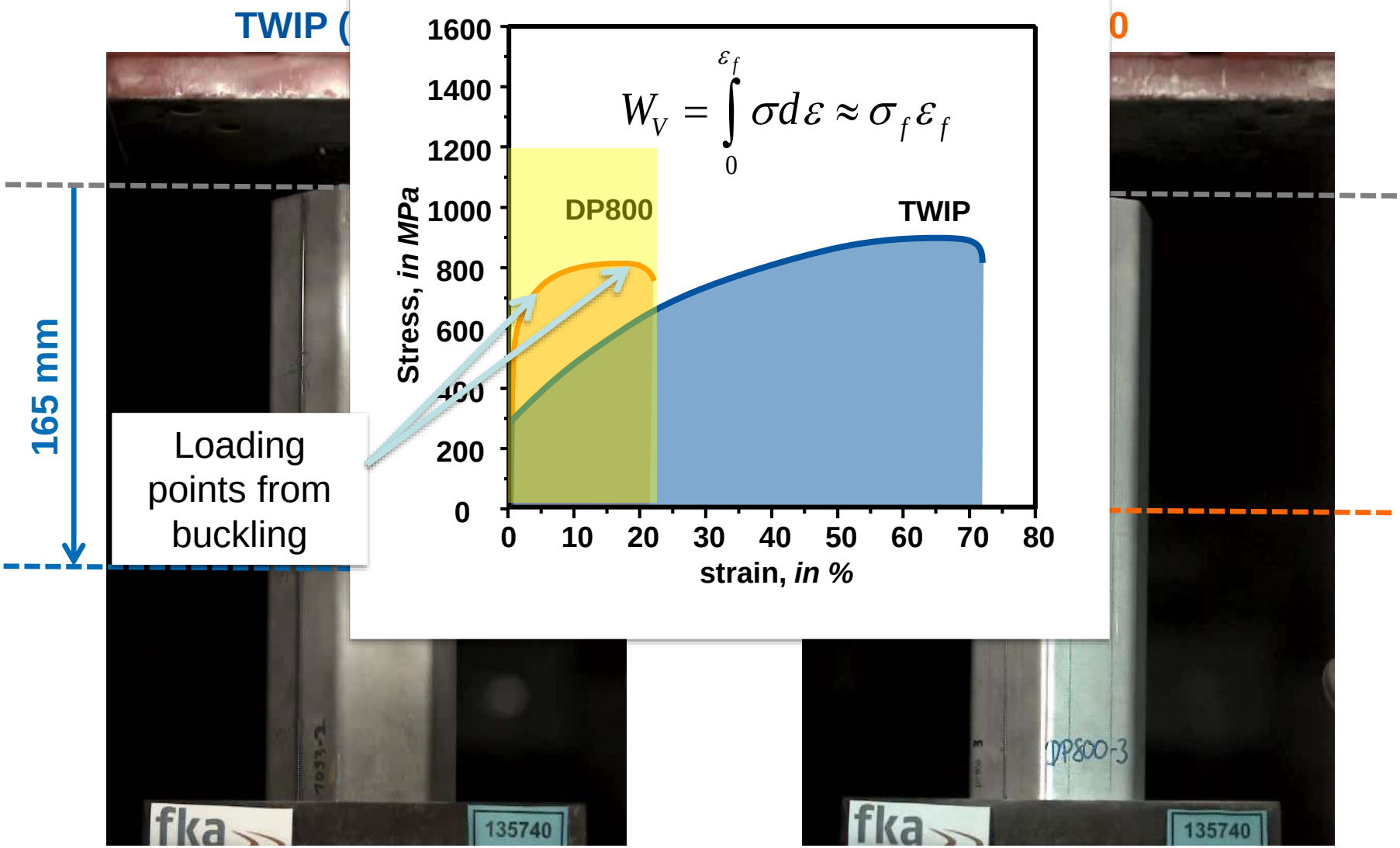

DFG SFB 761: M. Bambach, G. Hirt (RWTH)

1. What is Metastability Alloy Design and Segregation Engineering ?

2. **How is it done ?**

- Bulk: tune barriers & transformation driving forces
- **Confinement to lattice defects**
  Segregation & local displacive transformation

Fe-9%Mn, 450°C/6h

- Mn 11 at% isosurface
- Mn
- Fe

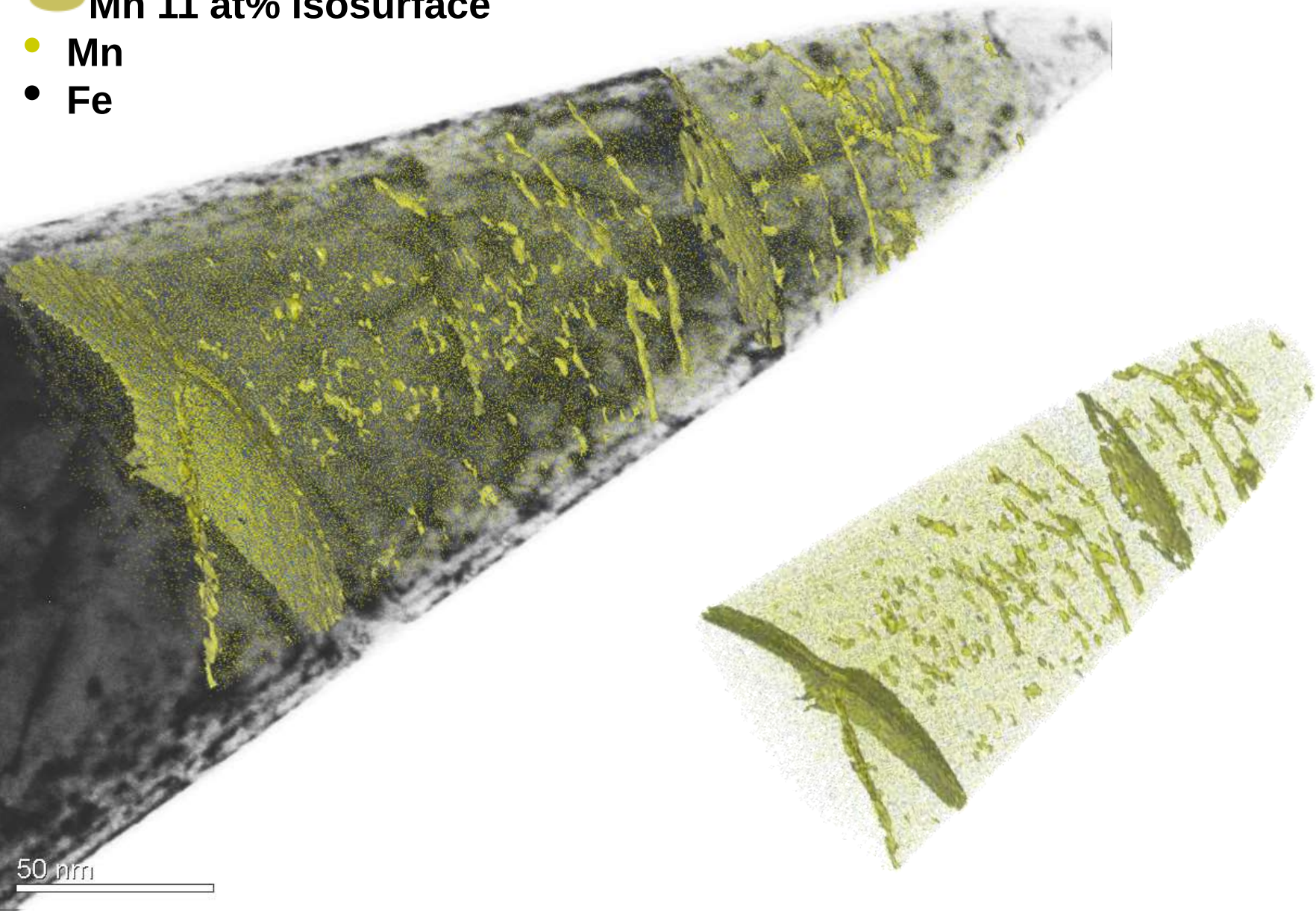

Kuzmina et al. Science 349, 1080 (2015)

Fe-9%Mn 450°C/6h, dislocation spinodal

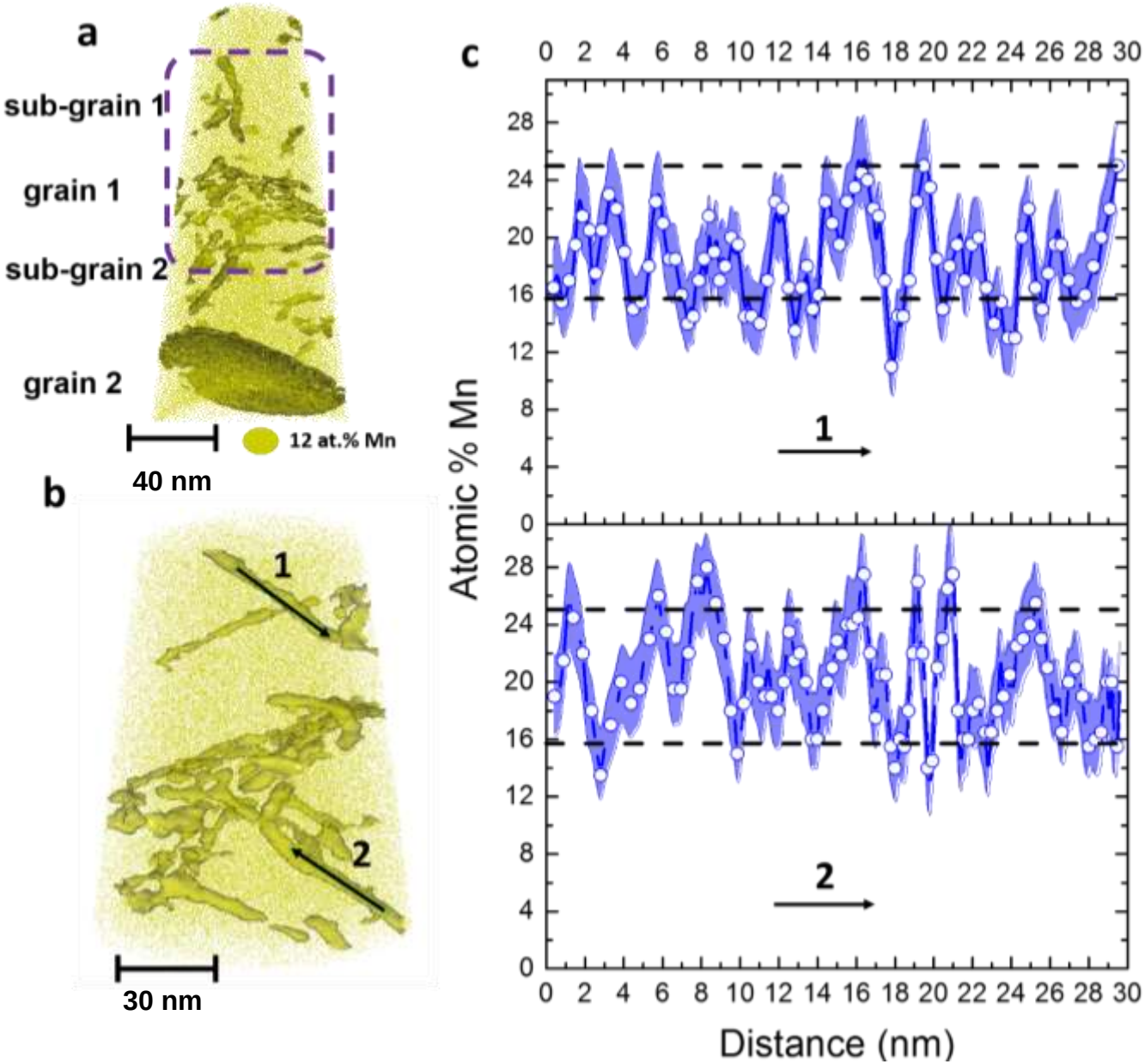

Austenite films in Fe-9Mn-3Ni-1.4Al (wt%): reversion steels

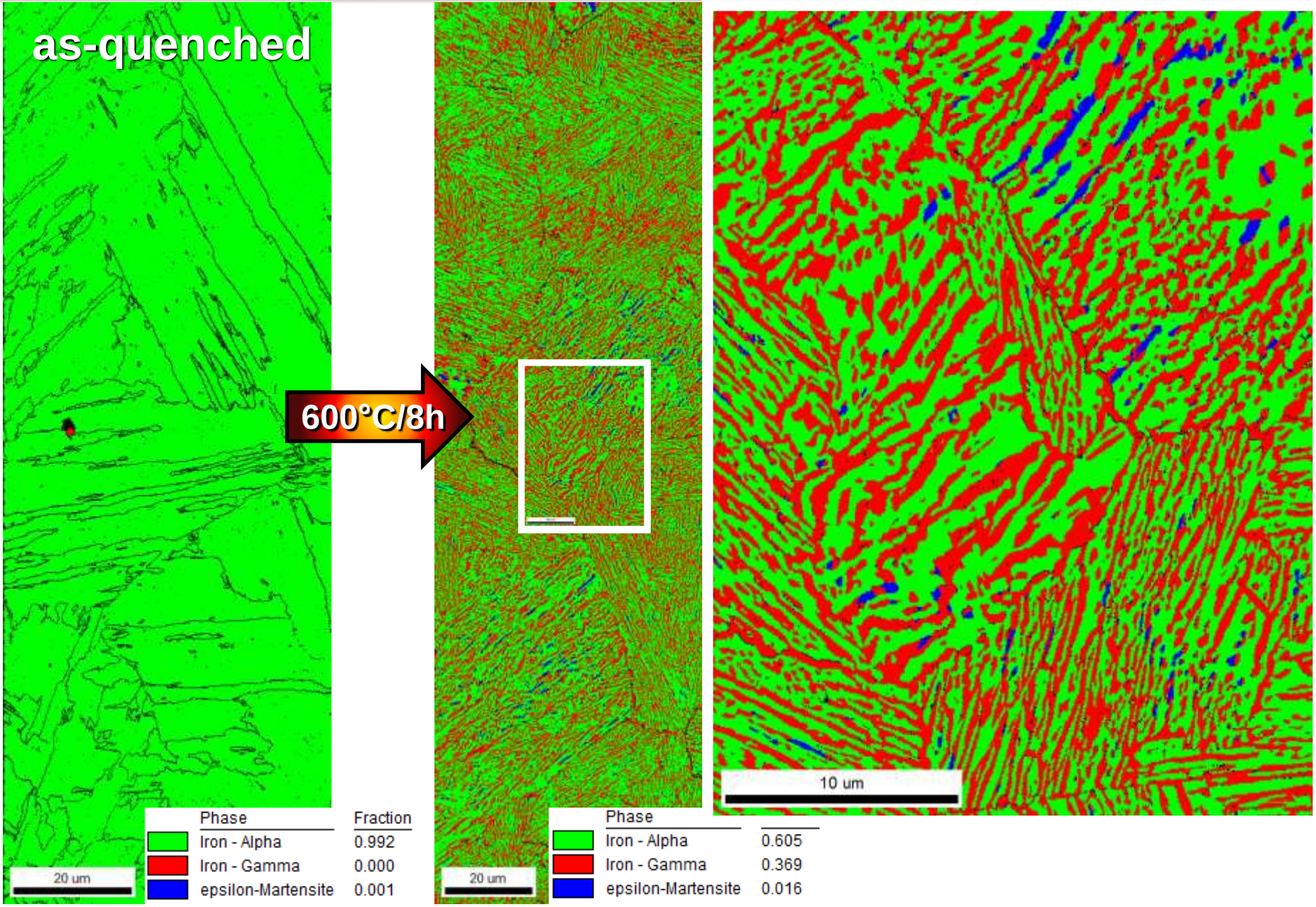

Wang (2015) Acta Mater 85, Raabe et al. Acta Mater. 61 (2013) 6132

Metastability alloy design towards bone – like metals

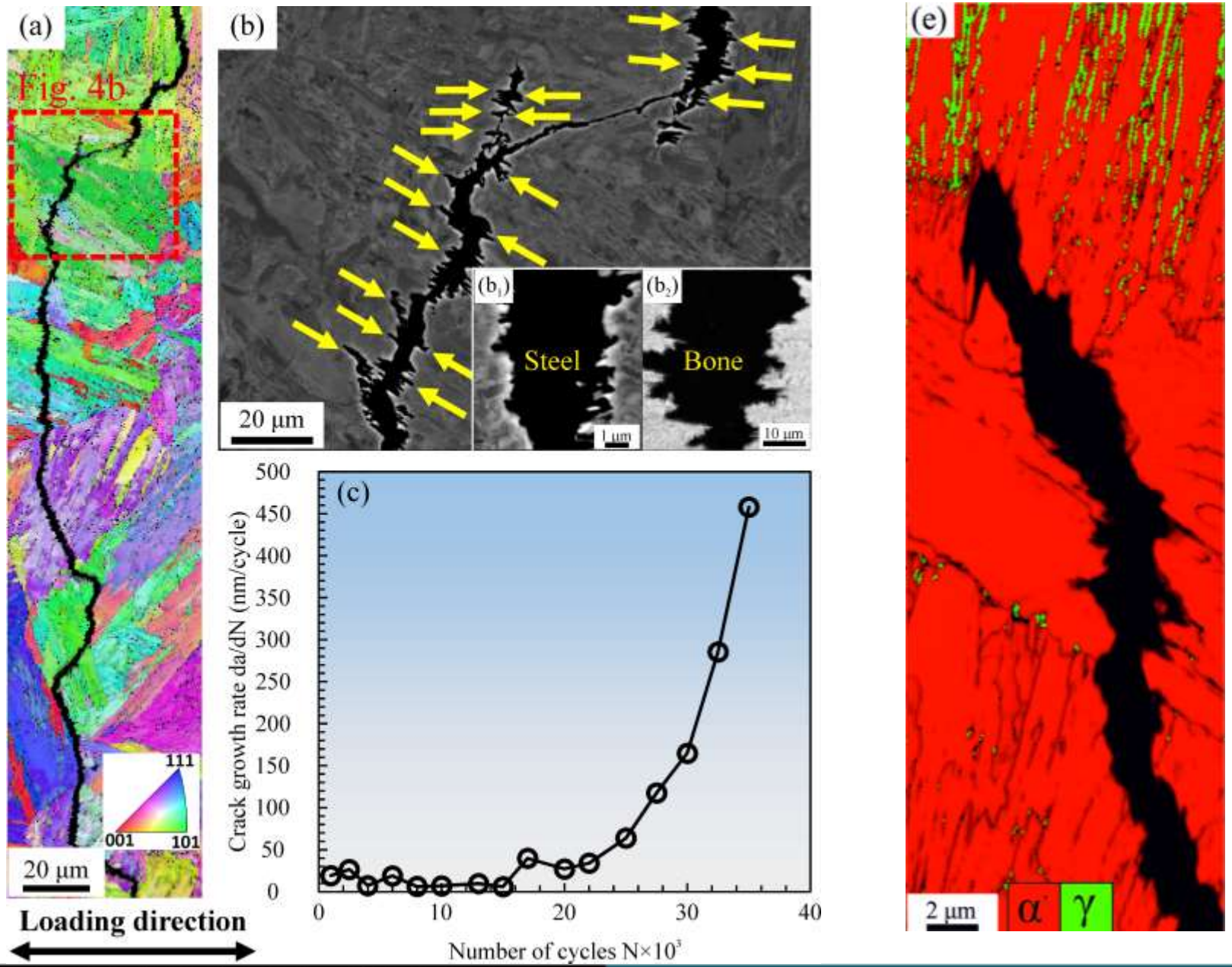

Koyama et al. Science 355 (2017); Wang (2015) Acta Mater 85

Metastability alloy design towards bone – like metals

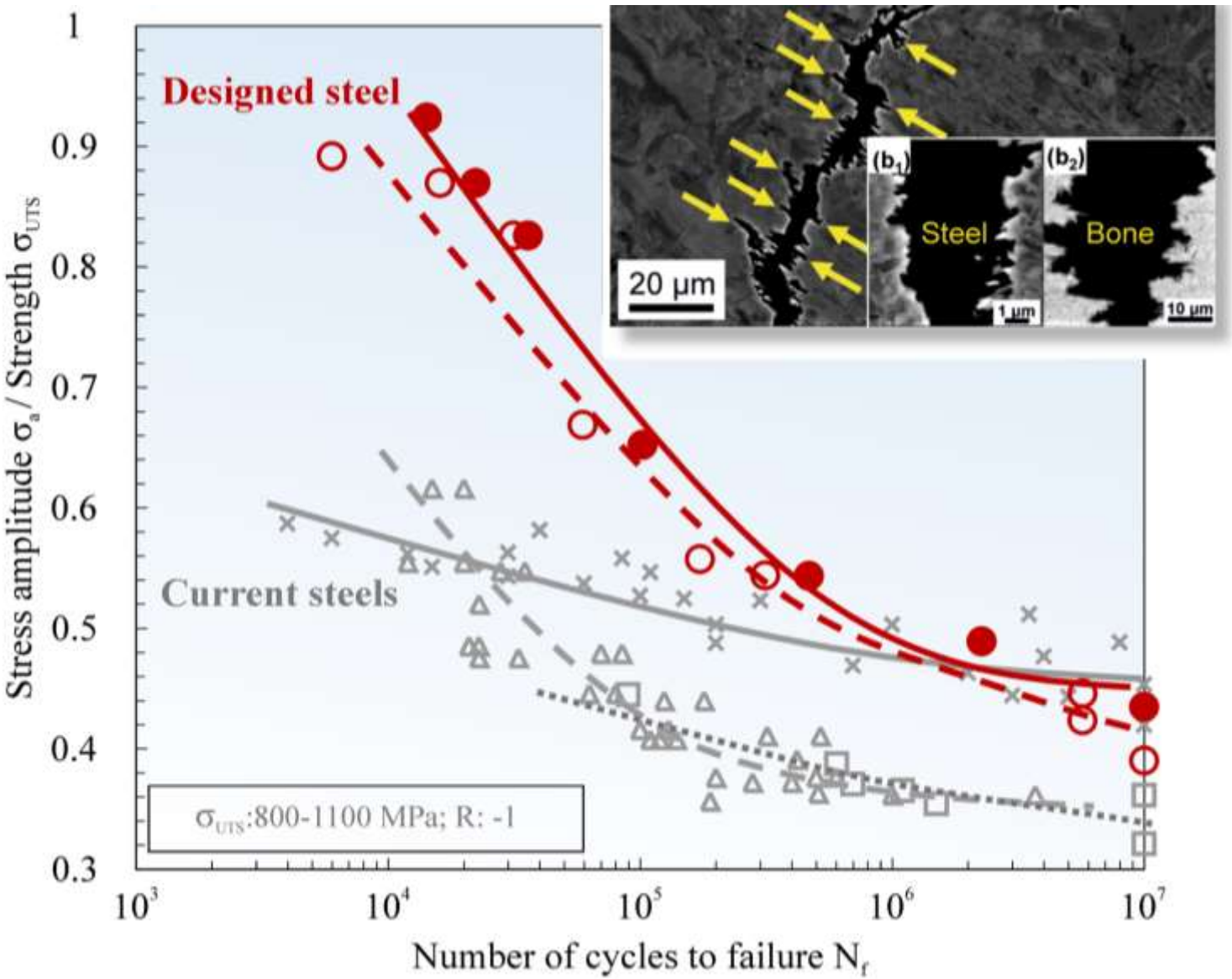

Koyama et al. Science 355 (2017)

Theory-guided design: non-iso concentration high entropy alloys

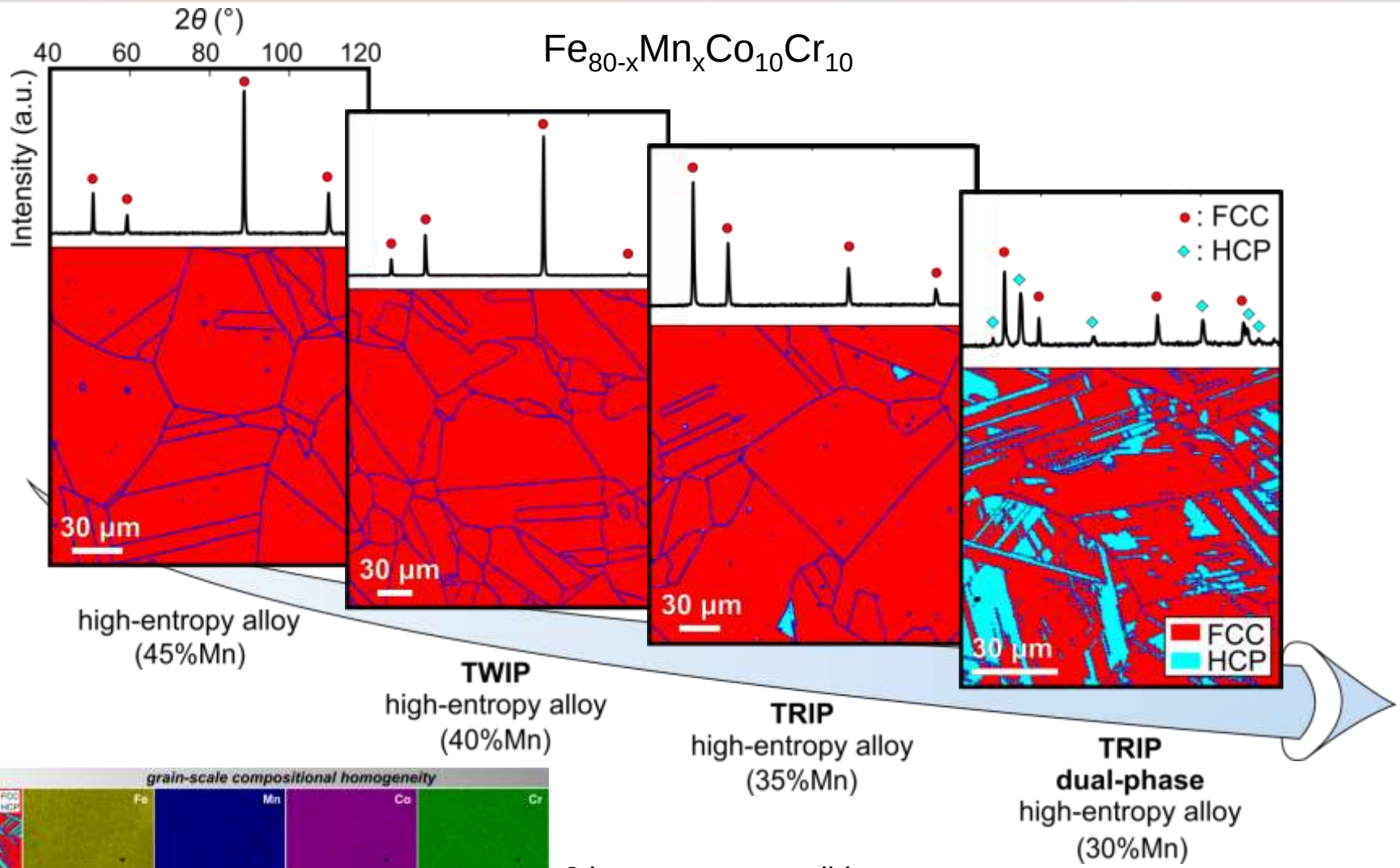

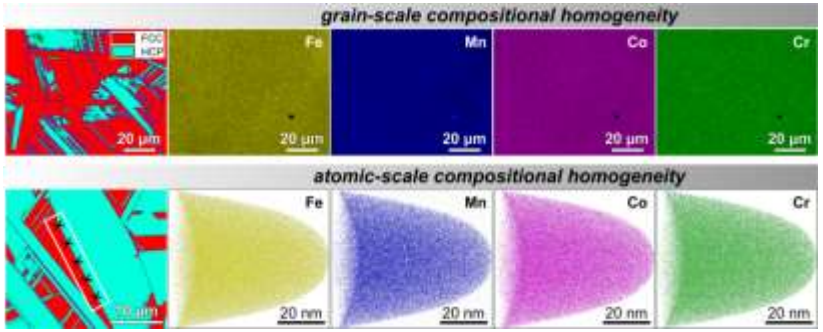

2 homogeneous solid solution HEA phases

Y. Deng et al. Acta Mater. 94 (2015) 124

Theory-guided design: non-iso concentration high entropy alloys

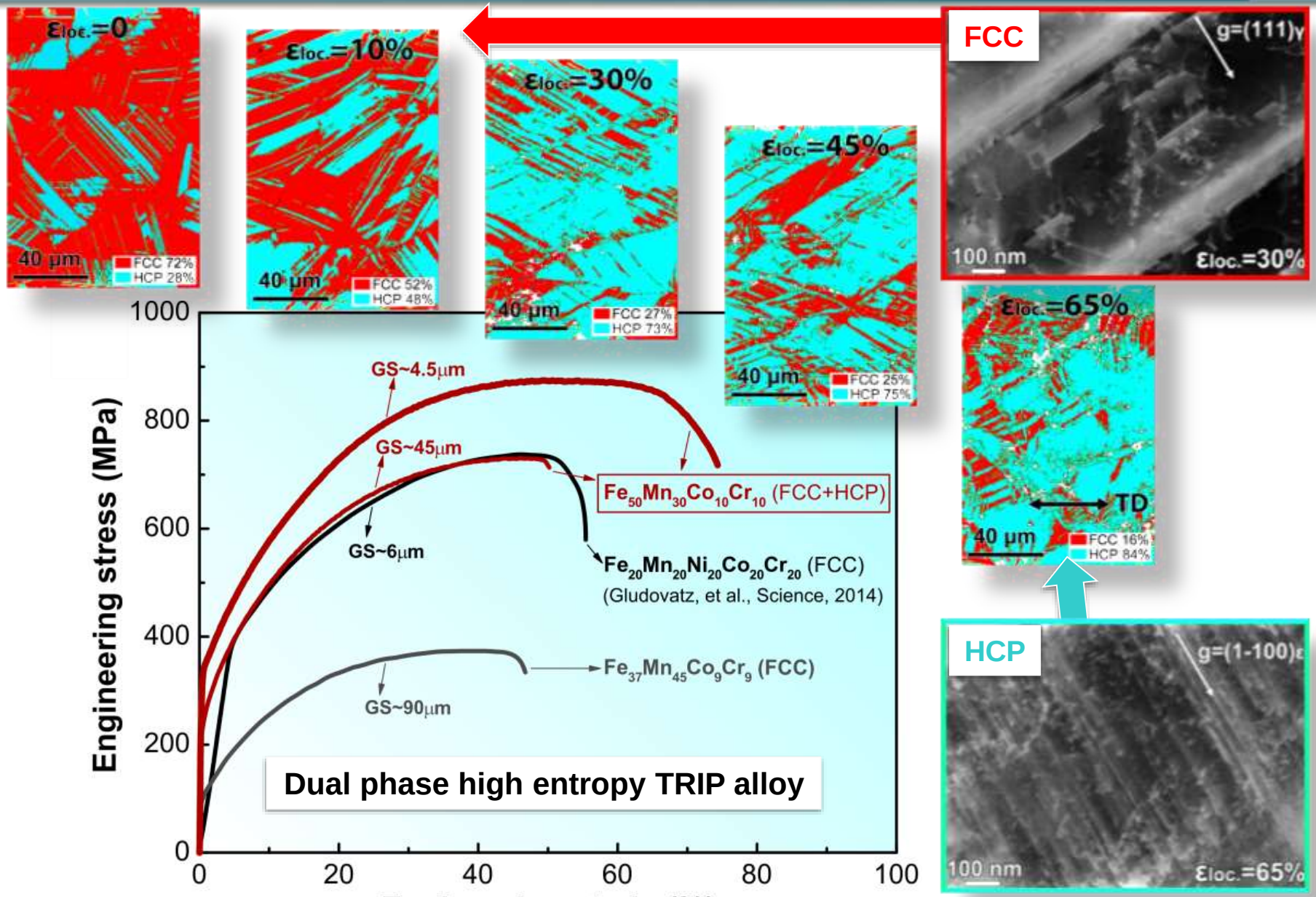

Z. Li et al. Nature 2016

Nanostructured bulk alloys by phase reversion: towards properties

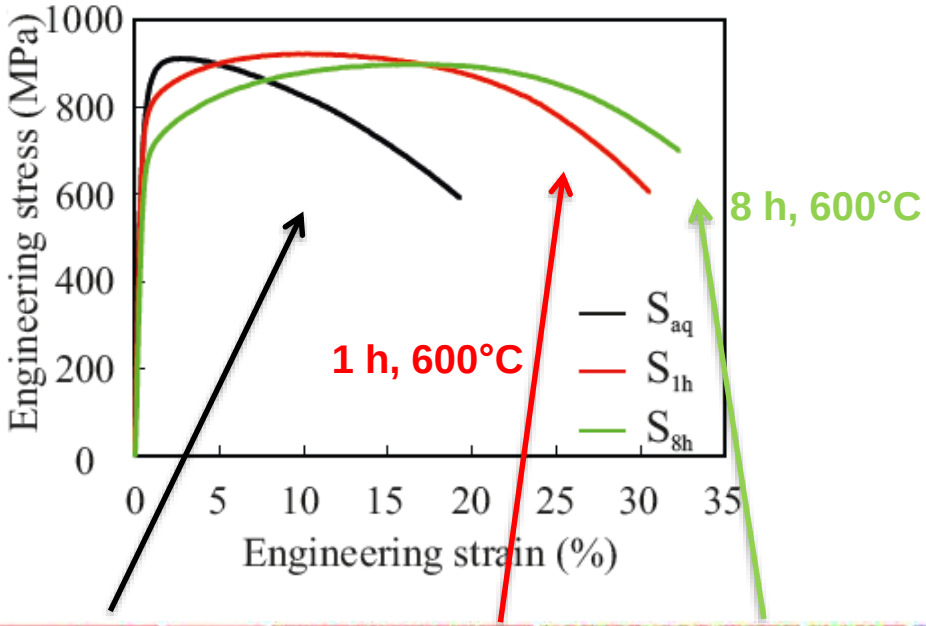

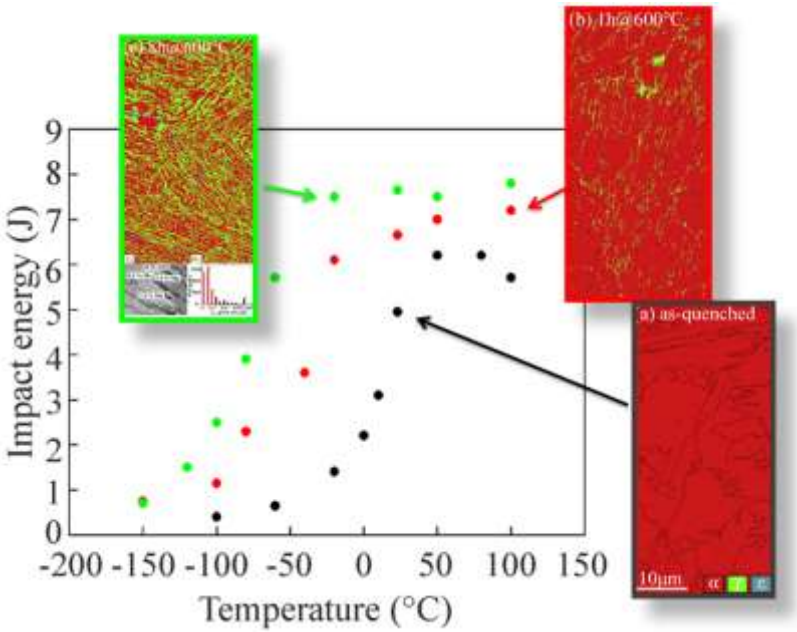

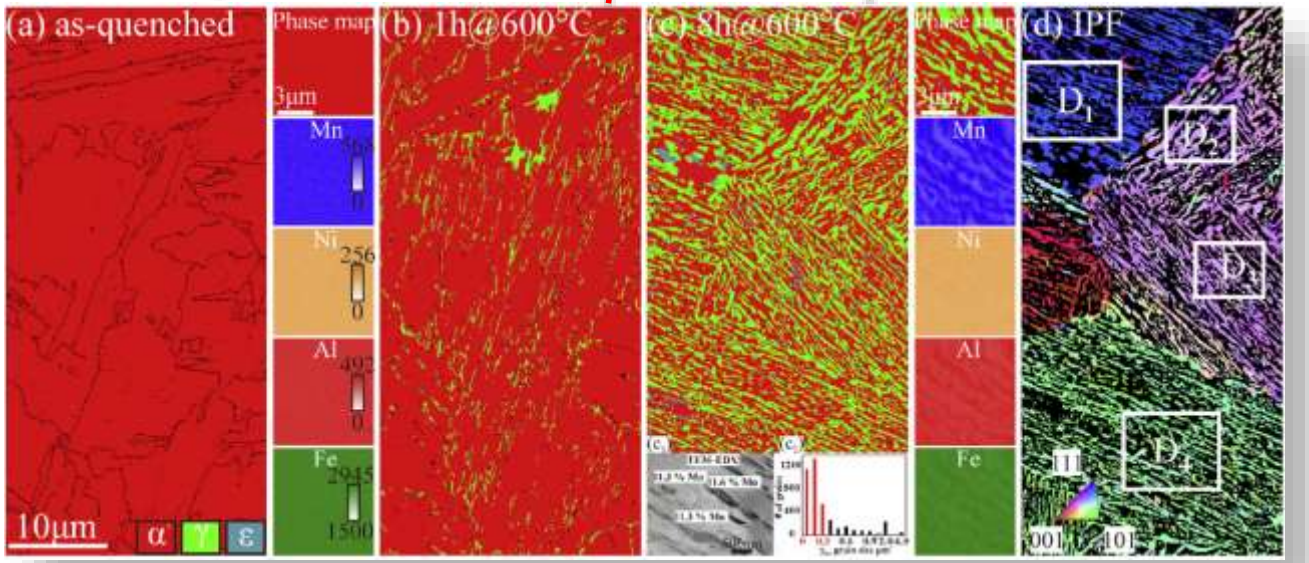

as quenched 1 h, 600°C 8 h, 600°C

Wang et al. Acta Mater. 79 (2014) 268;
Dmitrieva et al Acta Mater. 59 (2011) 364

Grain boundaries in Fe-9Mn

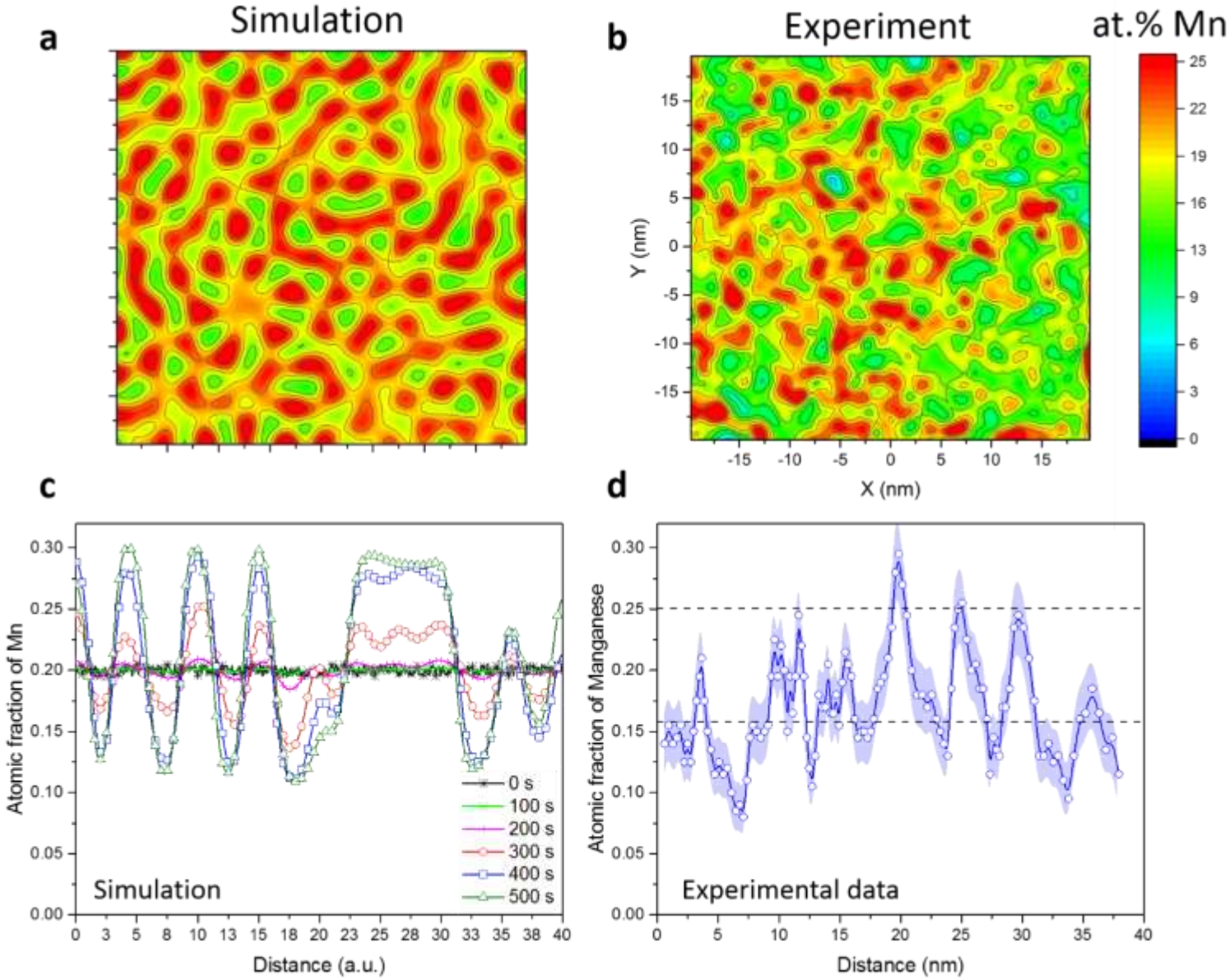

GB co-segreation in Cantor HEA

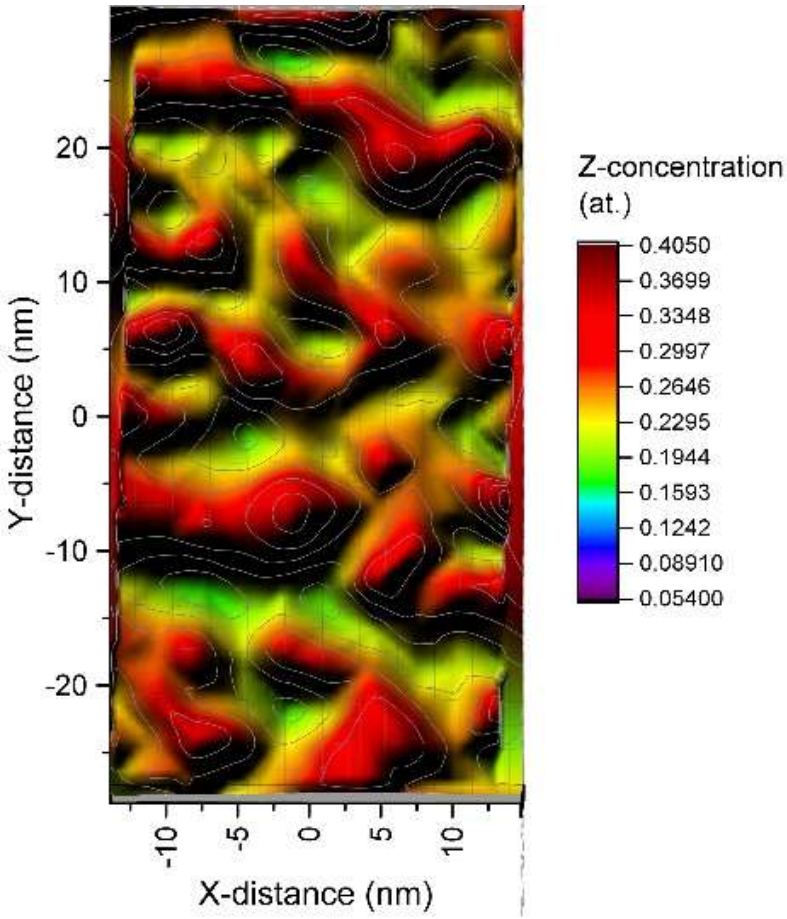

Ni in GB
450℃, 6h

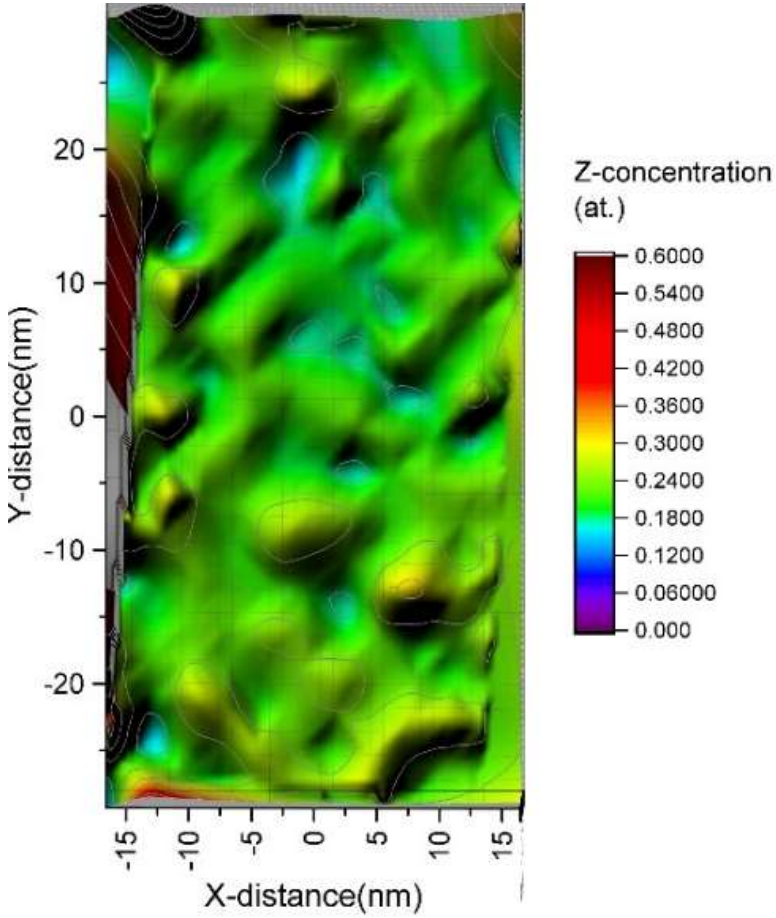

Mn in GB
450℃, 6h

Correlative Atom Probe and TEM (450°C/6h, Fe-9%Mn)

Grain boundaries and dislocations visible in both, TEM and APT

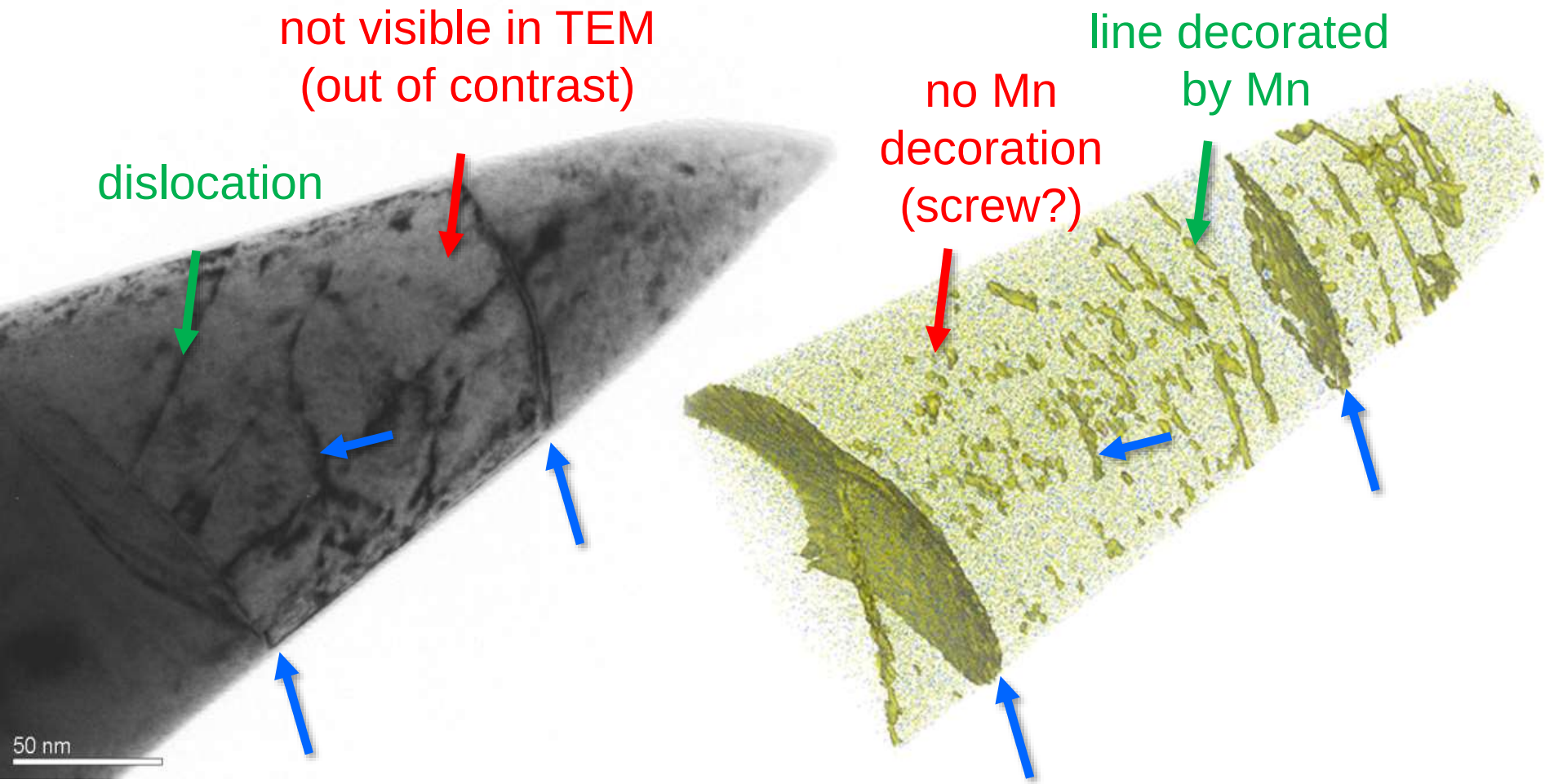

Method: Herbig et al. PRL (2014), Kuzmina et al. Science (2015), Li et al. PRL (2014), Jiang et al. Nature (2017), Herbig et al. Ultramic. (2015), Guo et al. PRL (2014)

9Mn-2Ni-0.15Al-1Ti-1Mo (wt.%), aged 450°C/65h

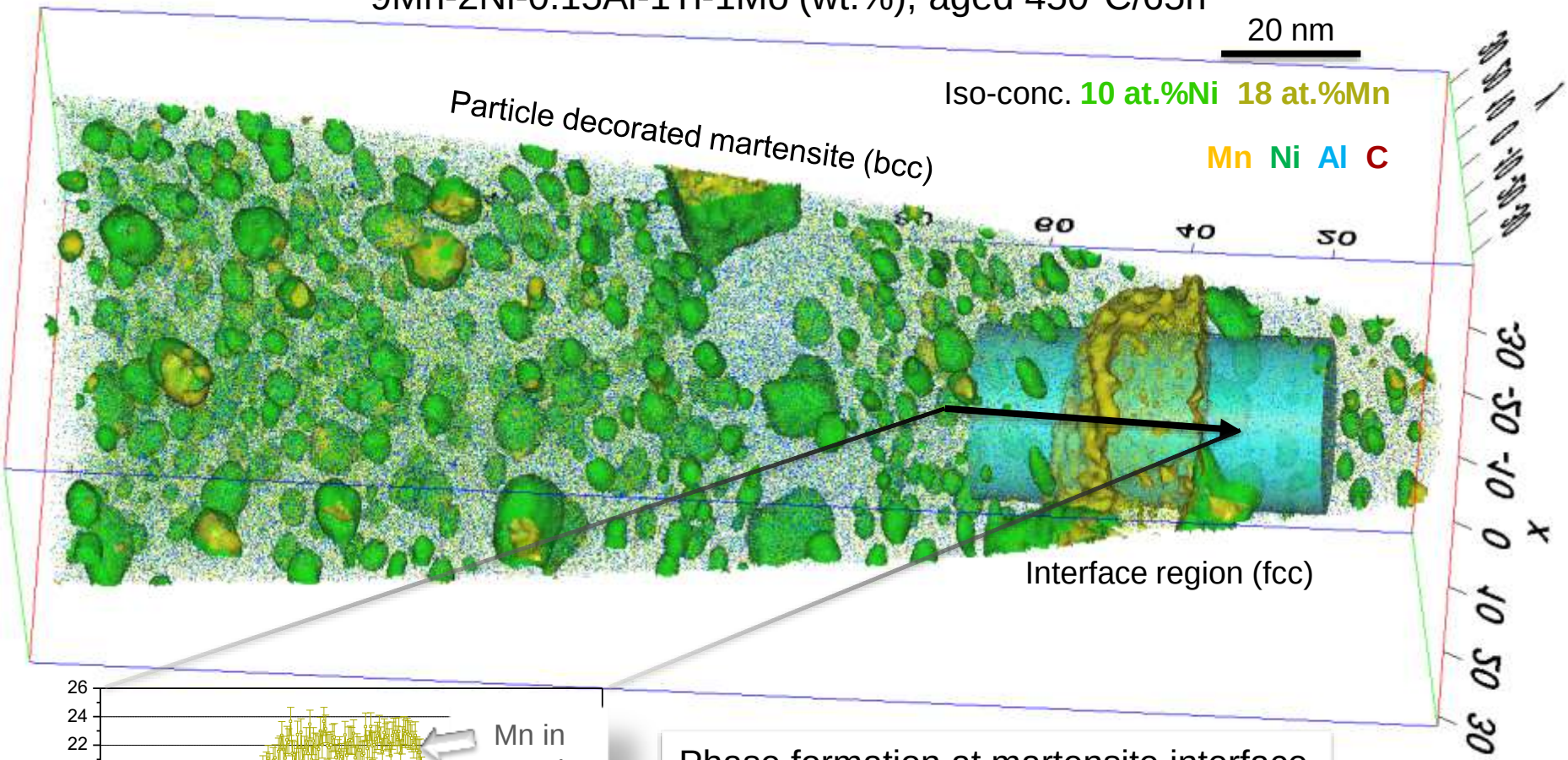

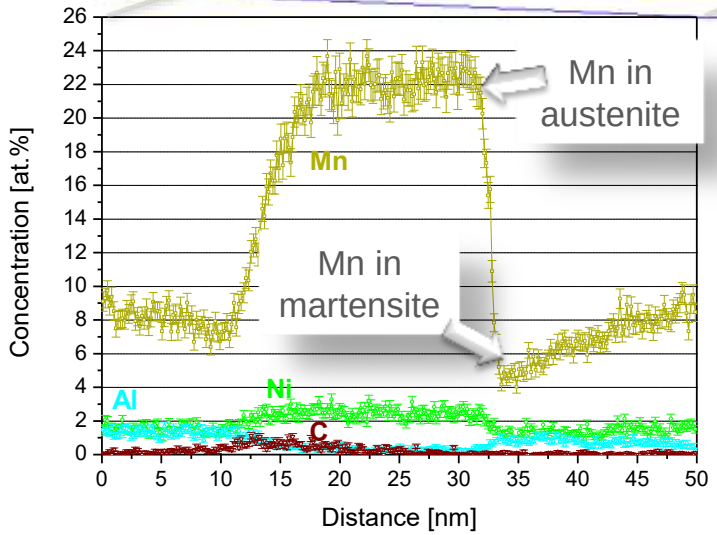

Phase formation at martensite interface

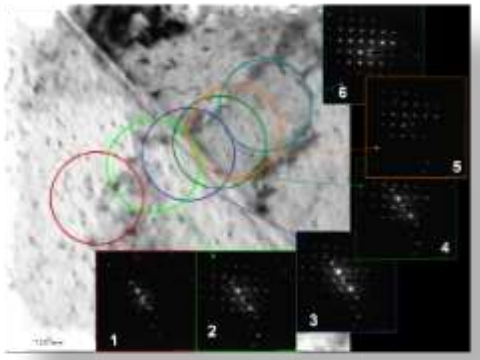

Raabe et al. Acta Mater. 61 (2013) 6132; Scripta Mater. 60 (2009) 1141